PERFORMANCE ANALYSIS OF MULTIHOP WIRELESS NETWORKS

（マルチホップ無線ネットワークの
特性解析に関する研究）

Nguyen Dang Khoa

Contents

Abstracts

Wireless communication has been considered as the most efficient mean of data transmission. We have been witnessed the breakthrough of wireless communication era in many manifolds, such as speech, coverage area, and stability. However, frequency bands, the resource to convey information wirelessly, are limited and expensive to be granted usage licenses.

Attaining the goals of ubiquitous wireless devices will require the future wireless networks stepping forward to overcome the scarcity and expensiveness of wireless frequency bands. Thus, the future wireless networks should evolve to utilize wireless frequencies more efficiently, such as cognitive relay network where non-license users are able to transmit data in the same frequency band that officially allocated to primary users. Subsequently, the transmit power of users in a cognitive network is limited and the performance is vulnerable to impairments of transceiver hardware.

This dissertation aims to analyze the performance of the cognitive relay network under the impact of transceiver hardware impairments. A case study of two-way cognitive relay network is given for further investigate the impact of transceiver hardware impairments on end-to-end outage performance and throughput. Furthermore, we provide a new relaying scheme in order to lessen the impact of transceiver hardware impairment and further boost the system performance. For the purposes, this dissertation is organized into five (5) chapters.

Chapter 1: *Introduction*. In this chapter, multihop wireless networks and the performance metrics are overviewed. In particular, the relay networks and cognitive relay networks are presented. Moreover, the general model of the practical transceiver hardware impairment is detailed for further analysis.

Chapter 2: *The impact of transceiver hardware impairments on cognitive relay networks*. By using the general hardware impairment model for the received signal, the closed forms of outage probability of the relay network with decode-and-forward (DF) and amplify-and-forward (AF) under the impact of transceiver hardware imperfection are derived. Based on these results, we provide further discussion on transceiver hardware selection guideline.

Chapter 3: *Case study: two-way cognitive relaying in energy harvesting wireless sensor networks*. A two-way relay wireless sensor network equipped with RF energy harvesting node is introduced. This network is aimed to be implemented in hazardous or remote areas where power supply for the relay node is difficult to maintain. In this chapter, we consider four configurations of the network with formed by combining two bidirectional relaying protocols and two wireless power transfer policies. The detailed performance analysis of outage probability and throughput of the case-study network with four configurations are presented. Based on the analysis, we provide performance comparison between the four and suggest the network configuration with the best performance.

Chapter 4: *Soft information relaying protocol*. The soft information relaying protocol is proposed and analyzed. The analysis shows that this relaying protocol can gradually reduce the impact of transceiver hardware impairment on cognitive relay networks. Hence, soft relaying protocol is considered as a solution for cognitive relay network with cost-effective wireless transceiver devices.

Chapter 5: *Overall conclusion*. An overall summary of the works presented in the above is provided in this chapter. Moreover, the future related work is also discussed.

The results in this dissertation acknowledge the impact of transceiver hardware impairment by presenting the reduction of outage probability and throughput of the cognitive relay network. It puts forward the consideration of including the impact of transceiver hardware impairments on wireless network performance analysis, especially for the cognitive networks of which the transmit power is limited.

Furthermore, a new relaying protocol, namely soft information relaying protocol, is proposed as a solution to lessen the impact of transceiver hardware impairment.

The analysis shows that the impact of transceiver hardware impairment in cognitive relay network is reduced in compared to conventional relaying schemes.

As a final point, we have provided a full picture of performance analysis for the cognitive relay network under the impact of transceiver hardware imperfection and the solution to reduce the performance loss by applying soft information relaying scheme. This research would contribute to boost the development of cognitive relay networks where frequency bands are used more efficiently.

List of symbols

α	time fraction of energy harvesting and information processing phase
$\bar{\eta}$	total noise at destination in soft information relaying protocol
$\bar{\eta}_D$	noise term of the received signal at destination from the relay
$\bar{\gamma}$	maximum transmit power per AWGN noise, equal to $\frac{I_P}{N_0}$
β	the scaling factor for the forward signal from the relay to the destination in soft information relaying
ε	power sharing fraction of the RF energy harvesting node
η	AWGN noise
η_d	AWGN noise at the destination
η_r	AWGN noise at the relay
$\frac{1}{\lambda_1}$	variance of h_1
$\frac{1}{\lambda_2}$	variance of h_2
$\frac{1}{\lambda_3}$	variance of h_3
$\frac{1}{\omega_1}$	variance of g_1
$\frac{1}{\omega_2}$	variance of g_2
$\frac{1}{\omega_3}$	variance of g_3
γ	instantaneous SNR function

γ_t	outage threshold
$\hat{x_D}$	the decoded signal at the destination in soft information relaying protocol
$\hat{x_R}$	the forward signal from relay to destination in soft information relaying protocol
κ_1	transceiver hardware impairment level of the source
κ_2	transceiver hardware impairment level of the sink
κ_A	aggregate transceiver hardware impairment level at node A
κ_B	aggregate transceiver hardware impairment level at node B
κ_d	aggregate transceiver hardware impairment level at the destination
κ_r	aggregate transceiver hardware impairment level at the relay
$\mathcal{CN}(0,\sigma^2)$	complex Gaussian variable with zero-mean and variance σ^2
$\mathcal{T}$	network throughput
μ	energy conversion efficiency of the rectification process
$\mu_{\tilde{\eta}}$	mean of the soft noise at relay
ν_1	gain of the complex channel g_1
ν_2	gain of the complex channel g_2
ν_3	gain of the complex channel g_3
ρ_1	gain of the complex channel h_1
ρ_2	gain of the complex channel h_2
ρ_3	gain of the complex channel h_3
$\sigma^2_{\tilde{\eta}}$	variance of the soft noise at relay
τ	distortion noise caused by transceiver hardware impairment
τ_1	transceiver hardware impairment distortion at the transmitter

τ_2	transceiver hardware impairment distortion at the receiver
τ_d	aggregate distortion noise caused by transceiver hardware impairment at the destination
τ_r	aggregate distortion noise caused by transceiver hardware impairment at the relay
τ_r	aggregate transceiver hardware impairment distortion at the destination
τ_r	aggregate transceiver hardware impairment distortion at the relay
ε_D	the impairment-noise-distortion at the destination, $\varepsilon_D \sim \mathcal{CN}(0, \kappa_D^2 P + N_0)$
ε_R	the impairment-noise-distortion at the relay, $\varepsilon_R \sim \mathcal{CN}(0, \kappa_R^2 P_S + N_0)$
Υ_{mabc}	the effective function that captures the effects of μ and α to the harvested energy E_H in MABC protocol
Υ_{tdbc}	the effective function that captures the effects of μ and α to the harvested energy E_H in TDBC protocol
$\widetilde{\eta}$	soft noise at relay node in soft information relaying protocol
$\widetilde{x}$	soft information that is calculated at the relay
B	bandwidth
C	AWGN channel capacity
$E_1(x)$	the exponential integral function of variable x
E_H	harvested energy at the RF energy harvesting relay node
$F_X(\cdot)$	cumulative distributed function (CDF) of random variable X
$f_X(\cdot)$	probability distributed function (PDF) of random variable X
G	amplify gain of the forwarding signal with AF scheme
g_1	source to primary receiver complex channel coefficient

g_2	relay to primary receiver complex channel coefficient
g_3	source B to primary receiver complex channel coefficient in two-way relay channel
h_1	source to relay complex channel coefficient
h_2	relay to destination complex channel coefficient
h_3	source to destination complex channel coefficient
I_P	maximum tolerance transmit power at the relay
L_R	log-likelihood ratio of the received signal at the relay
L_{RD}	log-likelihood ratio of the received signal at the destination from the relay
L_{SD}	log-likelihood ratio of the received signal at the destination from the source
N_0	variance of AWGN noise
P_A	transmit power at node A in the data processing phase
P_A^{EH}	transmit power at node A in the energy harvesting phase
P_B	transmit power at node B in the data processing phase
P_B^{EH}	transmit power at node B in the energy harvesting phase
P_R	transmit power at the relay in the data processing phase
P_S	transmit power at the source
R_A	data transmission rate at node A
R_B	data transmission rate at node B
T	the length of one relaying communication period in time domain
x	transmit signal at the source
y_d	received signal at the destination
y_r	received signal at the relay

List of Figures

List of Tables

1. Introduction

1.1 Motivations and objectives

Wireless technology has been developed in multiple aspects, such as increasing throughput, maximizing coverage area, and minimizing transmit power. Recently, multihop wireless networking has attracted many researchers since it is able to expand the traditional wireless communication link that is limited on the direct source – destination line–of–sight propagation link. Conventional wireless communication conveys data wirelessly from a source to a destination node via the direct link only. In multihop wireless networks, one or more intermediate wireless nodes, usually be called as relay nodes, are implemented to assist the data transmission between a source and a destination. The relay nodes receive and then forward the received data from the source to the destination, hence the wireless transmission from the source to the destination is possible even when the direct link is absent. Furthermore, multihop wireless networking technology can be deployed to extend the coverage area in a cost-efficient way due to the installation cost of a relay node is cheaper than that of a base station. In relay node, the distortion noise caused by transceiver hardware impairments has been known as an issue of degrading the system performance. However, there are lacking contributions on analyzing the impact of transceiver hardware distortion on the performance of multihop wireless networks. Especially in cognitive relay network where the transmit power is constrained to limit the interference noise to the primary-users. Subsequently, the impact of transceiver hardware impairment is required to be mentioned when analyzing performance of a cognitive relay network.

Motivated from the above reasons, this dissertation is intended to investigate the performance of cognitive relay network under the impact of transceiver hardware impairment. On the other hand, this is aimed to propose a solution to mitigate the

impact of transceiver distortion in order to allow cognitive relay network can be deployed at low cost with reasonable RF hardware components.

To offer the completive and rigorous understanding on cognitive relay networks, in certain parts of the thesis focus on scenarios like two way relaying and basic relay network topology with three wireless nodes, source, relay, and destination. However, the limitation of the transmit power of the primary user is strictly considered to fulfil the interference limit requirement of cognitive relay networks. Among the performance metrics, herein, the end-to-end reliability and the delay-limit transmission network throughput are mainly provided in this dissertation.

In the later of this chapter, relay networks and cognitive relay networks are overviewed. In addition, three main sources of distortion caused by transceiver hardware impairment and a general model of received signals under the impact of transceiver hardware impairment are presented.

1.2 Multihop wireless networks

1.2.1 Relay networks

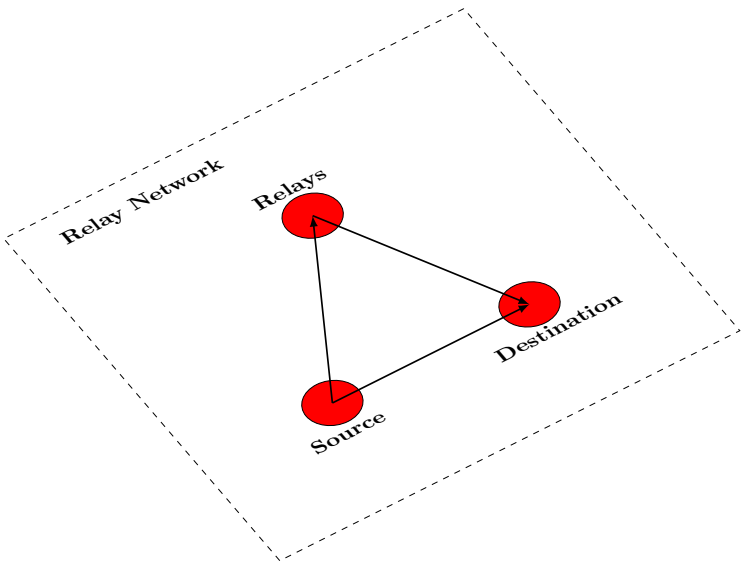

Figure 1.1: A three-node relay network topology

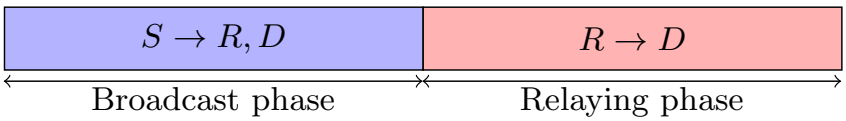

Figure 1.2: A data transmission cycle of the half-duplex relay network

A typical topology of a three-node relay network is depicted in Fig. 1.1 where data is transmitted from a source to a destination via two routes, the direct link and the relay link. In relay networks. data transmission process is often taken place into two timeslots. In the first timeslot, the source broadcasts the packet data to the relay and the destination. This phase is referred as broadcast phase. A specified data processing, which is called as relaying scheme, is applied to the received data at the relay. Then, the processed data is forwarded to the destination in the second timeslot, namely relaying phase, Fig. 1.2.

The information processing at the relay is different form the relaying protocol is deployed at the relay. The following relaying schemes are popular in literature and real applications.

1. **Amplify-and-Forward (AF)**: In AF relaying, the relay resembles the received analog signal in the broadcast phase, then it forwards an amplified version of that signal to the destination. Thus, the AF relaying is the simplest in implementation. However, it amplifies and retransmits not only the signal but also the noise to the destination. Hence, AF relay protocol offers the least performance improvement in compared to other relaying schemes due to the accumulated error issue.

2. **Decode-and-Forward (DF)**: The relay *regenerates* the received data in the first timeslot into a new clear data version by first demodulating the received signal. Then an error detecting code, such as cyclic redundancy check codes, and/or error correcting codes, for instance turbo codes, are applied. Subsequently, the new version of the received packet data is modulated and forwarded to the destination. DF relaying is able to offer a error-free of the forwarding signal to the destination. Hence, system performance is improving; and circuit complexity is increasing in compared to AF relaying scheme

3. **Demodulate-and-Forward (DemF)**: Unlike DF relaying, DemF only de-

modulates the received signal in the broadcast phase, then modulates it and forward to the destination. By demodulating the received signal, error in the first phase is avoided to be amplified before relaying to the destination. When the same modulation is utilized at both the source and the relay, the destination can combine two versions of signal from the two phases coherently.

A communication relaying protocol proposed for UMTS TDD mode have been included to a proposal for IEEE 802.16, 3GPP Opportunity Driven Multiple Access (ODMA) [1]. Recently, the relay based technology has been standardized in IEEE 802.16j, multihop relay-based wireless access network [2].

1.2.2 Cognitive relay networks

Relay networks is a cost effective solution for wireless transmission, however, the traffic among source – relay – destination can increase frequency bandwidth usage. Hence, the relay network is an inefficient utilization method in term of frequency spectrum which is expensive to be allocated usage licenses.

In Japan, the Ministry of Affairs and Communications (MIC) charges the utilization fee of 200 JPY a year per every base station which is deployed. On average, a 95.15 million JPY annual fee is charged for every 1 MHz of bandwidth used. In addition, frequency carriers are the limited resources [3]. Fig. 1.4 shows wireless frequency allocation in Japan for the frequency bands 500 MHz – 30 GHz for [4], where MWA (Mobile Wireless Access), FWA (Fixed Wireless Access), NWA (Nomadic Wireless Access), WLAN (Wireless Local Area Network), and PAN (Personal Area Network).

Cognitive radio network was proposed to overcome the scarcity of wireless frequency bands. It offers a new concept to improve spectrum utilization efficiency by allowing secondary users transmit data in the same frequency bands that officially allocated to primary users [5]. As depicted in Fig. 1.3, a typical topology of

[2]Source: H. Hojo, "Trends in wireless access system technology toward expanded broadband based on optical and wireless systems," NTT Tsukuba Forum 2007 Workshop Lectures 3, vol. 6, no. 5, May 2002.

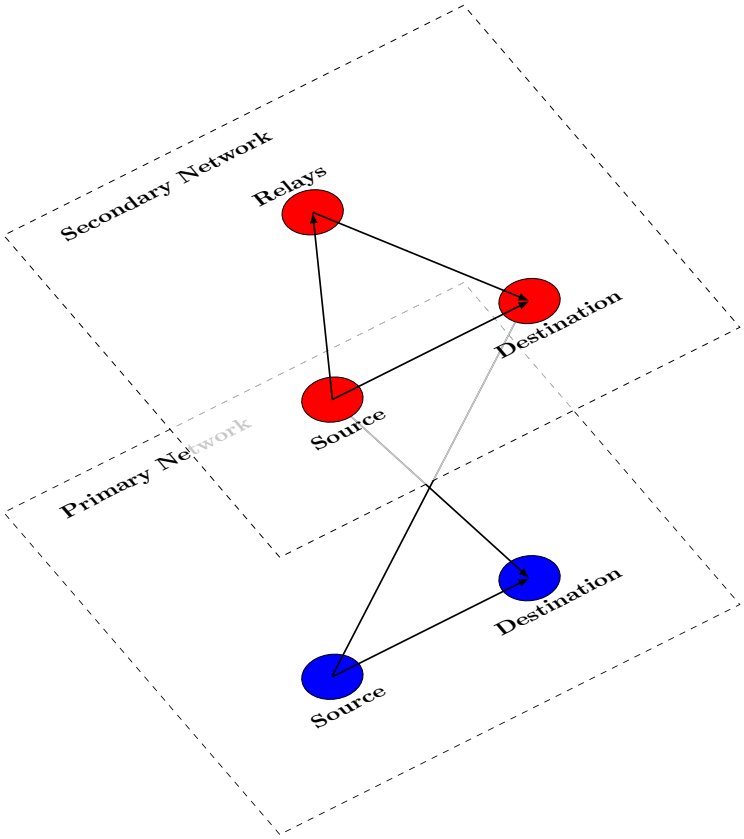

Figure 1.3: A cognitive relay network topology

a cognitive relay network consists of wirelss users that can be divided into two sub-networks, secondary and primary networks. Users in those networks can transmit data via the same carriers where only the primary users are officially allocated frequency license. The secondary users are allowed to transmit on the same frequency band providing that the transmissions cause interferences to the primary users under the limit. Consequently, secondary users' transmit powers is bounded. In this dissertation, the interference is caused by the transmission of secondary users to primary users is defined as *maximum tolerance interference*.

1.2.3 Performance metrics

In this dissertation, some performance metrics have been selected to evaluate the performance of the multihop network. These evaluation tools are described as the following.

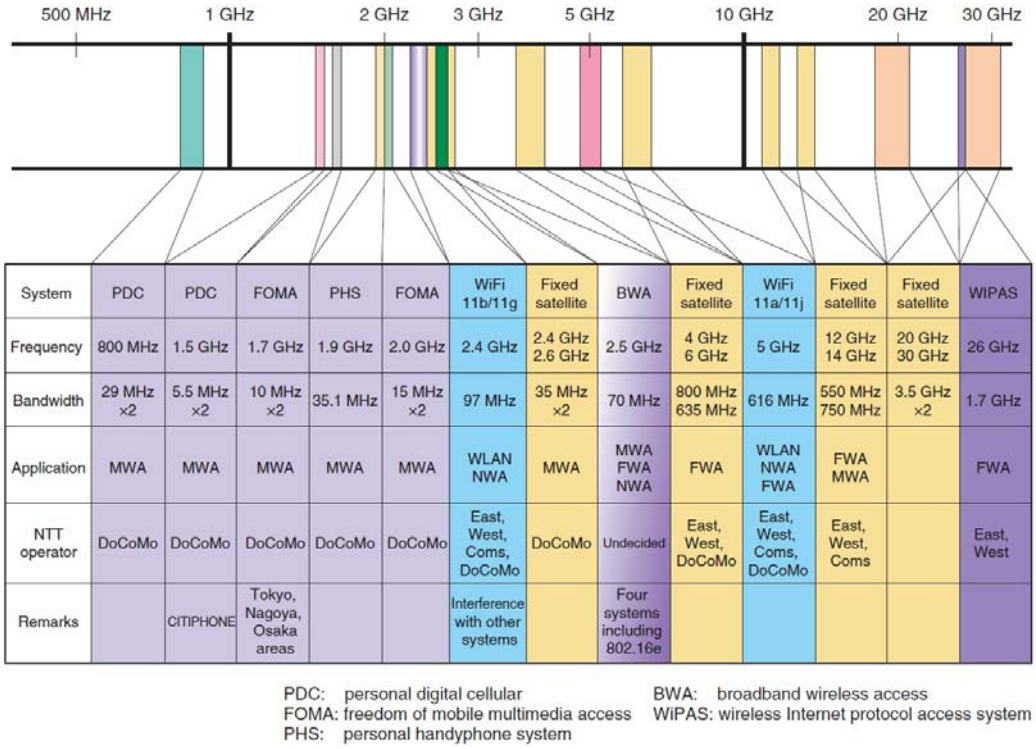

System	PDC	PDC	FOMA	PHS	FOMA	WiFi 11b/11g	Fixed satellite	BWA	Fixed satellite	WiFi 11a/11j	Fixed satellite	Fixed satellite	WIPAS
Frequency	800 MHz	1.5 GHz	1.7 GHz	1.9 GHz	2.0 GHz	2.4 GHz	2.4 GHz 2.6 GHz	2.5 GHz	4 GHz 6 GHz	5 GHz	12 GHz 14 GHz	20 GHz 30 GHz	26 GHz
Bandwidth	29 MHz ×2	5.5 MHz ×2	10 MHz ×2	35.1 MHz	15 MHz ×2	97 MHz	35 MHz ×2	70 MHz	800 MHz 635 MHz	616 MHz	550 MHz 750 MHz	3.5 GHz ×2	1.7 GHz
Application	MWA	MWA	MWA	MWA	MWA	WLAN NWA	MWA	MWA FWA NWA	FWA	WLAN NWA FWA	FWA MWA		FWA
NTT operator	DoCoMo	DoCoMo	DoCoMo	DoCoMo	DoCoMo	East, West, Coms, DoCoMo	DoCoMo	Undecided	East, West, DoCoMo	East, West, Coms, DoCoMo	East, West, Coms		East, West
Remarks		CITIPHONE	Tokyo, Nagoya, Osaka areas			Interference with other systems		Four systems including 802.16e					

PDC: personal digital cellular
FOMA: freedom of mobile multimedia access
PHS: personal handyphone system
BWA: broadband wireless access
WiPAS: wireless Internet protocol access system

Figure 1.4: Frequency allocation to wireless systems in Japan [2]

1. End-to-end reliability: Reliable transmission is an important criteria of a wireless network. A successful transmission is acknowledged when the SNR of the received data at the destination is larger than a per-defined SNR threshold which is chose to ensure the received data can be retrieved to the original data correctly. The end–to–end reliability is also called as outage probability which is measured as the probability of the successful transmissions per the total transmissions. Hence, we aim to provide the knowledge of the end-to-end reliability of all the networks will be mentioned in this thesis.

2. Network throughput: Besides the end-to-end reliability probability, the network throughput is another important system performance factor. Network throughput is determined as the total data rates that are transmitted to all terminals in a network. In this dissertation, the network throughput in the context of delay–limited transmission is studied.

1.3 RF transceiver hardware impairments

Nowadays, consumer wireless products operate at high carrier frequency of up to 6 GHz and planning to be implemented in mm-wave 60 GHz band for future wireless devices [6; 7]. RF transceiver hardware becomes a critical element to enable data transmission properly via mm-wave wireless channel. Despite the important role of the RF transceiver in the wireless device, its effects on system performance, such as outage probability and throughput, have been discussed rarely in literature due to the complexity of analysis model. In this section, we would like to brief the main sources of hardware impairments in RF transceivers and then develop a simplified general model of transceiver hardware impairment that can be used to investigate the impact of transceiver hardware impairments on the performance of wireless systems.

1.3.1 Sources of distortion in RF transceiver

Among many sources of RF transceiver hardware impairments that can cause errors on the transmission and reception data, phase noise, IQ imbalance and nonlinearities are the majority problems. The brief introduction of those impairments will be explained in the following.

1.3.1.1 Phase noise

The impairment in hardware of RF oscillator has been considered as the main source that limits the performance of SISO OFDM systems. In [8], the author has explained the mechanisms that phase noise of the RF oscillator contaminates SNR and BER of an OFDM signal. The degradation of BER of OFDM signal with M-PSK and M-QAM over AWGN channel that caused by the presence of carrier frequency offset and carrier phase noise in a certain oscillator has been studied in [9]. Furthermore, the effects of phase noise on SNR of an OFDM system has been evaluated in [10]. In particular, the degradation of BER performance that caused by phase noise is sharply in low-cost systems [7]. Hence, the impact of phase noise has to be included

on the performance and analysis of high carrier frequency wireless systems.

1.3.1.2 IQ imbalance

In order to produce low-cost wireless devices, the concept of *direct conversion* has been introduced in [11]. Direct conversion method simplifies the transceiver hardware architecture by reducing the external intermediate frequency filter and image rejection filter [12]. Consequently, the direct conversion transceiver offers cost saving in compared to the conventional transceiver. However, it introduces some drawbacks, such as DC offset through self-mixing, $\frac{1}{f}$ noise and the large performance loss in IQ mismatch situation. IQ imbalance causes a severe impact in MIMO wireless system where multiple transceivers are implemented. Many studies on compensation the impacts of IQ imbalance in direct conversion transceivers have been introduced, for instance a data-aided estimation and compensation method for frequency independent at transmitter and receiver [13]. Despite the significant suppression of the influence of IQ mismatch in the new proposed direct conversion method, the impact of IQ imbalance in RE transceiver to wireless system performance is unavoidable.

1.3.1.3 Nonlinearities

Realistic transceiver includes A/D converter and low-noise amplifier at the receiver side as well as D/A converter and digital amplifier at the transmitter side. These circuits are the main sources that reason nonlinearities of transmitting and receiving wireless signals. However, these nonlinearities are being replaced by the approximately linear model in performance analysis. Hence, the effects of nonlinearities in BER and throughput have been negligible. In MIMO system, to tackle the negative influence of nonlinearities on the performance, the spatial shifting technique has been inaugurated to lower the PAPR in space division multiplexing modulation based MIMO system. In this technique, the transmit data vector is rearranged so that the subparts of the transmit data branches produce the smallest overall PAPR. The benefits of spatial shifting technique on reducing nonlinearities effects have been presented in [13]. Nevertheless, the impact of nonlinearities to wireless sys-

tem performance is inescapable.

1.3.2 Transceiver hardware impairment model

Although transceiver hardware impairments cause multiple side effects to wireless system performance, these impacts have been excluded in data transmission model of literature on performance analysis. Consequently, the performance gap between analytical and realistic transceiver model of a wireless system is huge. In this dissertation, we utilize the general RF transceiver hardware impairment model that presented in [13] as the model of transmit and receive signal to narrow the simulation gap. This model is promoted to cover all the effects of hardware impairments in wireless transceiver in a compact form which is able to apply in performance analysis continently.

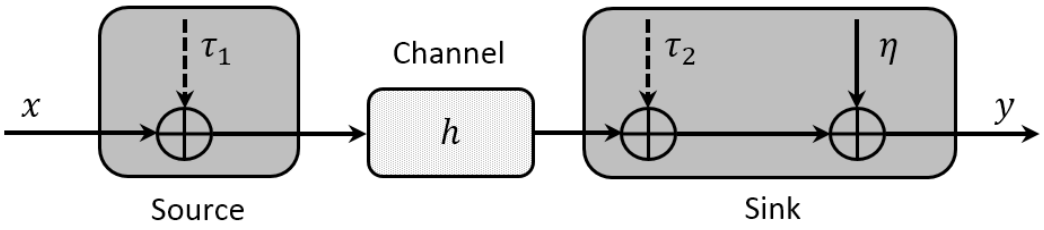

Figure 1.5: Transmission model with impairment.

First of all, we would like to give an overview of the model for transceiver hardware impairments of wireless nodes. We assume that the source transmits a complex signal $x \in \mathbb{C}$ with power P_x over the wireless channel with coefficient h to the sink. The transmission model is illustrated in Fig. 1.5. The signal experiences AWGN noise η. Practical transceiver impairments at the source distorts the signal x before it is emitted, whilst the imperfect transceiver hardware of the receiver distorts the received signal during the reception phase. Each source of distortion is represented by a different hardware model. Let τ_1, τ_2 be the *distortion powers* affecting the source and destination, respectively. τ_1 and τ_2 are complex random variables with normal distribution. The received signal can be succinctly expressed as

$$y = h(x + \tau_1) + \tau_2 + \eta. \tag{1.1}$$

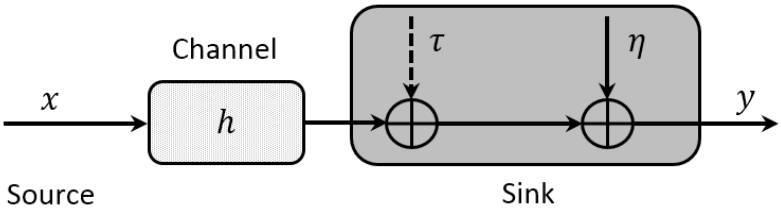

Figure 1.6: Transmission model with aggregate impairment.

$\tau_1 \sim \mathcal{CN}(0, \kappa_1^2 P_x)$ and $\tau_2 \sim \mathcal{CN}(0, \kappa_2^2 P_x |h|^2)$, as in [14]. κ_1, κ_2 are the *impairment levels* at the source and destination transceivers, respectively. Following [14], the distortion powers caused by transceiver impairments at the source and destination can be represented as an aggregate distortion power at the receiver, such that $\tau \sim \mathcal{CN}(0, \kappa^2 P_x)$, where $\kappa \triangleq \sqrt{\kappa_1^2 + \kappa_2^2}$ is the aggregate impairment level [14]. Then, the transmission model can be simplified as in Fig. 1.6, whereas equation (1.1) can be rewritten as

$$y = h(x + \tau) + \eta. \tag{1.2}$$

To this end, the received signal that modelled as (1.2) is used to describe the received signal at the receiver in the throughout of this dissertation.

2. Impact of Transceiver Hardware Impairments on Cognitive Network

Transceiver hardware impairments are the distortion noise sources that can degrade the performance of wireless systems. In this chapter, we analyze the impacts of hardware impairments on the outage performance and throughput of the cognitive relay networks with amplify-and-forward (AF) and decode-and-forward (DF) relaying protocol under the transmit power limit constraint. We derive the exact expressions that quantify the impacts of transceiver hardware impairments on the outage performance and throughput of the networks and corroborate the results by simulations. It is shown that the impacts of transceiver impairments are nonlinear and increase proportional to the increment of hardware impairment levels. Interestingly, we find that the cognitive relay networks with AF protocol is more susceptible to transceiver hardware impairments than the DF protocol. Consequently, the DF cognitive relay networks provide better outage performance and throughput than the AF cognitive networks in the same system parameters.

2.1 Introduction

Cognitive networks allows non-licensed users to transmit their signals wirelessly on the same frequency spectrum that officially authorized to licensed-users. With cognitive networks, the valuable radio frequency bandwidth is utilized more efficiently. It is considered as a promising solution to combat the limited frequency spectrum in wireless communication [5; 15; 16]. However, the challenge of cognitive networks is the transmit power constrain in order to guarantee the quality-of-service

(QoS) of the secondary users while preserving primary user's performances. Recently, the use of relay nodes is proven to benefit wireless networks by improving coverage, reliability and QoS [17; 18]. To tackle the transmit power limitation, the concept of deploying relay nodes in the cognitive networks has attracted researchers both in academia [19; 20] and in industry [21]. The introduction of cognitive relay (CR) networks can exploit the advantages of relaying protocols and overcome the transmit power limitation to further boost the system performances.

Literature on analysis performance of CR networks have been increased rapidly in recent years; however, only ideal transceiver model was considered to analyze the outage probability (OP) and throughput of the system. In [22], the OP of decode-and-forward (DF) CR networks was reported with the constraint imposed on the interference suffered by the primary users. The work in [19] analyzed the performance of spectrum sharing amplify-and-forward (AF) in the existence of transmit power constrain and the interference from a primary transmitter. The OP of the cognitive DF networks over Nakagami-m fading was performed in [23]. In the mentioned research articles, the transceiver of the relay nodes were supposed to be flawless. Nevertheless, the practical transceiver hardware suffers from several types of impairments; such as, I/Q imbalance [24; 25], high power amplifier nonlinearities [26]. Recently, the impacts of hardware impairments to relay networks were provided in [27]. Undoubtedly, those impairments also degrade the system performances of the CR networks, especially when the power budget is high.

In this chapter, we present a detailed performance analysis of an DF/AF CR networks in the presence of transceiver imperfections by utilizing the generalized impairment model of [13]. The contribution of this study is to provide new closed-form expressions of OP and throughout of the DF/AF CR networks with transceiver hardware impairment model. Based on the analytical results, the networks designers will be able to predict the maximum level of hardware imperfections they can tolerate to achieve a predetermined performance.

The chapter is organized as follows. Section 2.2, the detail DF/AF CR networks and channel models in this chapter are presented. Section 2.3 and Section 2.4 provides detail derivation of the end-to-end signal-to-noise-distortion ratio (SNDR), the exact OP closed-forms and throughput of the CR networks with DF and AF re-

laying protocol. In Section 2.5, Monte-Carlo simulations are shown to validate our analysis. Furthermore, some design guidelines are also propounded in this section. Finally, conclusions are given in Section 2.6.

2.2 System and channel model

We consider a half-duplex dual-hop CR networks that is illustrated in Fig. 2.1. The secondary users of the networks consists of three communication nodes, a source node S, a destination node D, and a relay node R, whereas the $PU-Rx$ receiver is the only node of the primary networks. Each node in the networks is equipped with a single antenna. In the first hop, S broadcasts signal x to R; the received signal at R is processed with the DF or AF relaying algorithm, then it is forwarded from R to D in the second hop.

All channels of the cognitive relay networks are assumed as independence non-identical distributed Rayleigh fading. Fading channel coefficients h_1, h_2, g_1 and g_2 are complex Gaussian distributed with zero mean and variances $\frac{1}{\lambda_1}$, $\frac{1}{\lambda_2}$, $\frac{1}{\omega_1}$, and $\frac{1}{\omega_2}$, respectively. Additive noise terms at R and D are $\eta_r \sim \mathcal{CN}(0,N_0)$, and $\eta_d \sim \mathcal{CN}(0,N_0)$. It is assumed that there is no line-of-sight transmission link from S to D due to the high pathloss and shadowing effects.

In order to limit the interferences of the transmitted signals of the CR networks to the primary receiver Rx, the maximum allowable transmit power of the CR networks is defined as the peak of transmit power of the secondary users, which is denoted as I_P. The transmit powers at S and R are P_s and P_r, respectively. We note that the transmit powers have to be equal or smaller than I_P. We enable secondary users transmit with the maximum power, therefore, the effective transmit power at S and R are $P_s = \frac{I_P}{|g_1|^2}$ and $P_r = \frac{I_P}{|g_2|^2}$, respectively.

All the secondary user transceivers are modeled with the impairment model that is discussed in Chapter 2. The received signals at R and D are suffered from the aggregate distortion powers $\tau_r = \mathcal{CN}(0, \kappa_r^2 P_s |h_1|^2)$ and $\tau_d = \mathcal{CN}(0, \kappa_d^2 P_r |h_2|^2)$ where κ_r and κ_d are the exaggerate impairment levels at R and D, respectively.

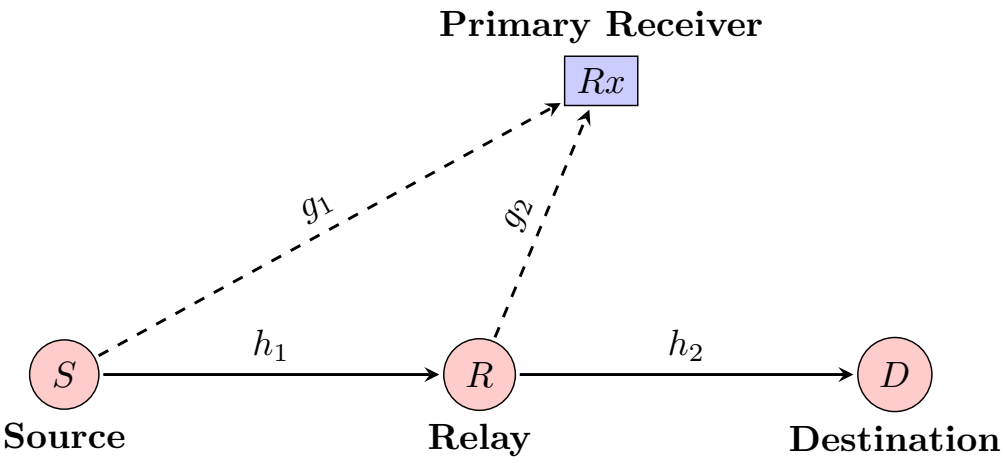

Figure 2.1: A cognitive half-duplex dual-hop relay network

2.2.1 DF CR networks: end-to-end SNDR

Let the CR network utilizes the DF relaying protocol where the received signal at R is decoded, re-encoded with a proper coding scheme before forwarded to D in the second phase of the transmission cycle. We assume that the decoder in R is flawless. Then, the received signal at R is expressed as

$$y_r = \sqrt{\frac{I_P}{|g_1|^2}} h_1 (x + \tau_r) + \eta_r. \tag{2.1}$$

Therefore, the instantaneous SNDR at R is given by

$$\gamma_1 = \frac{\frac{I_P}{N_0}|h_1|^2}{\frac{I_P}{N_0}|h_1|^2 \kappa_r^2 + |g_1|^2} = \frac{\bar{\gamma}|h_1|^2}{\bar{\gamma}|h_1|^2 \kappa_r^2 + |g_1|^2} \tag{2.2}$$

where $\bar{\gamma} = \frac{I_P}{N_0}$. Similarly, the received signal and the SINR at D respect to the transmission link $R \to D$ are given as

$$y_d = \sqrt{\frac{I_P}{|g_2|^2}} h_2 (y_r + \tau_d) + \eta_d \tag{2.3}$$

Then, the SNDR is deduced as

$$\gamma_2 = \frac{\bar{\gamma}|h_2|^2}{\bar{\gamma}|h_2|^2\kappa_d^2 + |g_2|^2}. \tag{2.4}$$

From (2.2) and (2.3), the end-to-end SNDR of the DF CR networks is given by

$$\gamma = \min(\gamma_1, \gamma_2). \tag{2.5}$$

2.2.2 AF CR networks: end-to-end SNDR

Let the CR network utilizes the AF relaying protocol where the received signal at R is amplified with a proper gain before being forwarded to D in the second phase of the transmission cycle. We assume that the decoder in R is flawless. Thus, the received signal at R is expressed as

$$y_d^{AF} = h_2 \left\{ G \left[\sqrt{\frac{I_P}{|g_1|^2}} h_1(x + \tau_r) + \eta_r \right] + \tau_d \right\} + \eta_d \tag{2.6}$$

where G is amplify gain of the AF relaying protocol. Let $\bar{\gamma} = \frac{I_P}{N_0}$, the amplify gain of the AF CR networks is characterized as

$$\frac{1}{G^2} = |g_2|^2 \left[\frac{|h_1|^2}{|g_1|^2}(1 + \kappa_r^2) + \frac{1}{\bar{\gamma}} \right]. \tag{2.7}$$

Substituting (2.7) into (2.6) with $\zeta_1 = \bar{\gamma}\frac{|h_1|^2}{|g_1|^2}$ and $\zeta_2 = \bar{\gamma}\frac{|h_2|^2}{|g_2|^2}$, the end-to-end SNDR of the AF CR networks is then given as

$$\rho = \frac{\zeta_1\zeta_2}{\zeta_1\zeta_2\kappa^2 + \zeta_1(1 + \kappa_r^2) + \zeta_2(1 + \kappa_d^2) + 1}. \tag{2.8}$$

2.3 End-to-end reliability analysis

2.3.1 Useful lemmas

Before stepping into the analysis, some useful lemmas will be shown and proofed. Notation that a, b. b_1, b_2, c and d are the positive scalars; X and Y are two independent non-identical exponential distributed non-negative RVs with zero means and variances $\frac{1}{\lambda_x}$ and $\frac{1}{\omega_y}$, respectively.

Lemma 2.1. *Let W_1 be a function of X, where $W_1 \triangleq \frac{aX}{bX+c}$.Then, the CDF of W_1 is given by*

$$F_{W_1}(\gamma_t) = \begin{cases} F_X\left(\frac{c\gamma_t}{a-b\gamma_t}\right) & \text{if} \quad 0 \leq \gamma_t \leq \frac{a}{b}, \\ 1 & \text{if} \quad \gamma_t \leq \frac{a}{b}. \end{cases} \tag{2.9}$$

Lemma 2.2. *Let W_2 be a function of X and Y, where $W_2 \triangleq \frac{aX}{Y}$. Then, the CDF and PDF of W_2 are respectively given by*

$$F_{W_2}(\gamma_t) = 1 - \left(1 + \frac{\omega_y}{a\lambda_x}\gamma_t\right)^{-1} \tag{2.10}$$

$$f_{W_2}(\gamma_t) = \frac{\omega_y}{a\lambda_x}\left(1 + \frac{\omega_y}{a\lambda_x}\gamma_t\right)^{-2}. \tag{2.11}$$

Lemma 2.3. *Let W_3 be a function of X and Y where $W_3 \triangleq \frac{aX}{abX+Y}$. Then, the CDF of W_3 is given by*

$$F_{W_3}(\gamma_t) = \frac{\omega_y\gamma_t}{\omega_y\gamma_t + (1-b\gamma_t)a\lambda_x}. \tag{2.12}$$

Proof. From the definition of the CDF of a random variable, we have

$$\begin{aligned} F_{W_3}(\gamma_t) &= Pr\left(\frac{aX}{abX+Y} \leq \gamma_t\right) \\ &= 1 - Pr\left(Y \leq X\frac{a-b\gamma_t}{\gamma_t}\right) \\ &= 1 - \int_0^\infty F_Y\left(X\frac{a-b\gamma_t}{\gamma_t}\right) f_X(x)dx \\ &= \int_0^\infty \exp\left(-\frac{a-b\gamma_t}{\omega_y\gamma_t}x\right)\frac{1}{\lambda_x}\exp\left(-\frac{x}{\lambda_x}\right)dx. \end{aligned} \tag{2.13}$$

The result of the integration in (2.13) yields to (2.12). □

Lemma 2.4. *Let W_4 be a function of X and Y, which is defined as*

$$W_4 = \frac{XY}{dXY + b_1X + b_2Y + 1}. \tag{2.14}$$

Then, the CDF of W_4 is given by

$$\begin{aligned} F_{W_4}(\gamma_t) &= 1 - \int_0^\infty \left[1 - F_X\left(\frac{b_2\gamma_t}{1-d\gamma_t} + \frac{\frac{b_1b_2\gamma_t^2}{1-d\gamma_t} + z}{z(1-d\gamma_t)}\right)\right] \\ &\quad \times f_Y\left(z - \frac{b_1z}{1-d\gamma_t}\right)dz. \end{aligned} \tag{2.15}$$

Proof. CDF of W_4 is defined as $F_{W_4} = Pr\{W_4 \leq \gamma_t\}$. Applying the rule of total probability conditioned on Y, (2.15) yields to

$$\begin{aligned} F_{W_4}(\gamma_t) &= \int_0^\infty Pr\{W_4 \leq \gamma_t|Y\} f_Y(y)dy \\ &= 1 - \int_0^\infty \left(1 - Pr\{W_4 \leq \gamma_t|Y\}\right) f_Y(y)dy \\ &= \int_{\frac{b_1\gamma_t}{1-d\gamma_t}}^\infty \left[1 - F_X\left(\frac{(b_2X+1)\gamma_t}{Y(1-d\gamma_t) - b_1\gamma_t}\right)\right] f_Y(y)dy. \end{aligned} \tag{2.16}$$

Let $z = Y - \frac{b_1\gamma_t}{1-d\gamma_t}$ and substitute z to (2.16). The integration in (2.16) yields to

(2.15). □

2.3.2 Outage performance analysis methodology

Outage performance of the CR networks is the probability that the end-to-end SNDR is less than a given threshold γ_t.

$$OP(\gamma_t) = Pr\{SNDR_{end-to-end} \leq \gamma_t\}. \quad (2.17)$$

In order to characterize the OP of the DF/AF CR networks, we aim to find the cumulative distributed function (CDF) of the end-to-end SNDR functions corresponding to the DF or AF protocol that are described in (2.5) and (2.8), respectively. Let us denote that $F(\cdot)$ and $f(\cdot)$ are the CDF and the probability distributed function (PDF) of a random variable. The CDFs of the end-to-end SNDR and the exact OP expressions of the DF/AF CR networks are derived in the next the subsections.

2.3.3 Outage performance of the CR DF network

In (2.5), γ_1 and γ_2 are two independent random variables, hence the CDF of end-to-end SNDR is given by

$$F_\gamma(\gamma_t) = F_{\gamma_1}(\gamma_t) + F_{\gamma_2}(\gamma_t) - F_{\gamma_1}(\gamma_t)F_{\gamma_2}(\gamma_t). \quad (2.18)$$

Lemma 2.3 enables us to characterize the CDF of $F_{\gamma_1}(\gamma_t)$ and $F_{\gamma_2}(\gamma_t)$ respectively as

$$F_{\gamma_1}(\gamma_t) = \frac{\omega_1\gamma_t}{\omega_1\gamma_t + (1-\kappa_r^2\gamma_t)\bar{\gamma}\lambda_1} \quad (2.19)$$

$$F_{\gamma_2}(\gamma_t) = \frac{\omega_2\gamma_t}{\omega_2\gamma_t + (1-\kappa_d^2\gamma_t)\bar{\gamma}\lambda_2}. \quad (2.20)$$

The exact OP of the DF CR networks is obtained by plugging (2.19) and (2.20) into

(2.18), which is expressed as

$$OP_{exact}^{DF}(\gamma_t) = \frac{\omega_1\gamma_t}{\omega_1\gamma_t+a_1}+\frac{\omega_2\gamma_t}{\omega_2\gamma_t+a_2}-\frac{\omega_1\gamma_t\omega_2\gamma_t}{(\omega_1\gamma_t+a_1)(\omega_2\gamma_t+a_2)} \quad (2.21)$$

where $a_1 = (1-\kappa_r^2\gamma_t)\bar{\gamma}\lambda_1$ and $a_2 = (1-\kappa_d^2\gamma_t)\bar{\gamma}\lambda_2$.

2.3.4 Outage performance of the CR AF network

Lemma 2.2 enables us express the CDFs and PDFs of ζ_1 and ζ_2 respectively as

$$F_{\zeta_j}(\gamma_t) = 1-\left(1+m_j\gamma_t\right)^{-1} \quad (2.22)$$

$$f_{\zeta_j}(\gamma_t) = m_j\left(1+m_j\gamma_t\right)^{-2} \quad (2.23)$$

where $m_j = \frac{\omega_j}{\bar{\gamma}\lambda_j}$ and $j \in \{1,2\}$. The OP of the AF CR networks is then expressed as

$$OP_{exact}^{AF}(\gamma_t) = 1-\int_0^{\infty}\left[1-F_{\zeta_1}\left(\frac{b_2\gamma_t}{1-d\gamma_t}+\frac{\frac{b_1b_2\gamma_t^2}{1-d\gamma_t}+z}{z(1-d\gamma_t)}\right)\right] \times f_{\zeta_2}\left(z-\frac{b_1z}{1-d\gamma_t}\right)dz \quad (2.24)$$

where $b_1 = (1+\kappa_r^2)$, $b_2 = (1+\kappa_d^2)$ and $d = (1+\kappa^2)$. Using the Lemma 2.4, the exact OP of AF CR networks is thus yielded to

$$OP_{exact}^{AF}(\gamma_t) = 1-\frac{\bar{\gamma}^2\Xi_2+AB\gamma_t(\Delta+b_1b_2\gamma_t)\Xi_1}{\Xi_2^2} \quad (2.25)$$

where $A = \frac{\omega_1}{\lambda_1}$, $B = \frac{\omega_2}{\lambda_2}$, $\Delta = 1-d\gamma_t$, and

$$\Xi_1 = \ln\frac{AB\Delta\gamma_t(\gamma_t+b_1b_2\gamma_t)}{\bar{\gamma}^2}-\ln\left(\Delta+\frac{Bb_1\gamma_t}{\bar{\gamma}}\right)-\ln\left(\Delta^2+\frac{Ab_2\Delta\gamma_t}{\bar{\gamma}}\right)$$

$$\Xi_2 = \Delta\bar{\gamma}^2+(Bb_1+Ab_2)\bar{\gamma}\gamma_t-AB\gamma_t.$$

2.4 Throughput analysis

Let us analyze the networks throughput in the context of delay-limited transmission. We assume that the source S transmits information to destination D at a fixed communication rate. The transmission rates at S is given as $R_S = \log_2(1+\gamma_t)$ [bits/s/Hz], where γ_t is the outage performance threshold. The networks throughput is measured as the throughput of the transmission link that can sufficient transmit data to the destination at the given rate. Hence, the networks throughput, $\mathcal{T}$, is established as

$$\mathcal{T}(\gamma_t) = R_S(1-OP(\gamma_t)) \tag{2.26}$$

where $OP(\gamma_t)$ is the end-to-end outage probabilities at the destination of the transmission link. The system throughput of cognitive DF networks is obtained by substituting the end-to-end outage probability at D given in (2.21) into (2.26)

$$\mathcal{T}_{DF}(\gamma_t) = \log_2(1+\gamma_t)\left[\frac{\omega_1\gamma_t}{\omega_1\gamma_t+a_1}+\frac{\omega_2\gamma_t}{\omega_2\gamma_t+a_2}-\frac{\omega_1\gamma_t\omega_2\gamma_t}{(\omega_1\gamma_t+a_1)(\omega_2\gamma_t+a_2)}\right] \tag{2.27}$$

$$= R\left[\frac{\omega_1\gamma_t}{\omega_1\gamma_t+a_1}+\frac{\omega_2\gamma_t}{\omega_2\gamma_t+a_2}-\frac{\omega_1\gamma_t\omega_2\gamma_t}{(\omega_1\gamma_t+a_1)(\omega_2\gamma_t+a_2)}\right]. \tag{2.28}$$

Likewise, the system throughput of the cognitive AF networks is obtained by substituting the end-to-end outage probability at D given in (2.25) into (2.26).

$$\mathcal{T}_{AF}(\gamma_t) = \log_2(1+\gamma_t)\left[1-\frac{\bar{\gamma}^2\Xi_2+AB\gamma_t(\Delta+b_1b_2\gamma_t)\Xi_1}{\Xi_2^2}\right] \tag{2.29}$$

$$= R\left[1-\frac{\bar{\gamma}^2\Xi_2+AB\gamma_t(\Delta+b_1b_2\gamma_t)\Xi_1}{\Xi_2^2}\right]. \tag{2.30}$$

2.5 Numerical results and discussion

In this section, the numerical results of the OP and throughput of the AF/DF CR networks are presented. The network nodes are arranged in Cartesian coordinates in which node S is located at the origin. Node R and D are placed along the $x-$ *axis* where R is in between S and D. Distance from S to D is normalized to unity.

The primary receiver $PU - Rx$ is freely positioned on the plane. We consider the case where the coordinates of S, R, D and $PU - Rx$ are $(0;0)$, $(0;0.4)$, $(0;1)$ and $(0.8;0.8)$, respectively.

The relation between the transmitted and received power with distance d is given by the decaying path loss model d^{-2}. The outage threshold $\gamma_t = 3$ is used to obtain the numerical results of outage probability and throughput. The aggregate impairment levels of R and D are similar, hence $\kappa^2 = \kappa_r^2 = \kappa_d^2$, $\kappa^2 \in \{0.05, 0, 1, 0.15\}$. The maximum allowable transmit power per AWGN noise is $\frac{I_P}{N_0} \in [0, 50]$ [dB].

Table 2.1: Simulation parameters for the cognitive relay network

Name	**Value**
Fading model	Rayleigh
Path loss model	Exponential d^{-2}
Outage threshold	$\gamma_t = 3$
Hardware impairment level	$\kappa_r^2, \kappa_d^2, \kappa^2 \in 0.05, 0.1, 0.15$
Maximum transmit power	$\frac{I_P}{N_0} \in [0, 50]$

Figure 2.2 portrays the impacts of hardware impairments to the OP of the AF/DF CR networks. As shown in the figure, the analysis and simulation results are identical in all cases, and the OPs of the DF/AF CR networks where the equal of transmit power are nonlinearly increasing to the hardware impairment level κ^2 increments. This is because the distortion powers are the proportional functions of κ^2. The results also indicate that the OP of the AF CR networks is more susceptible to the impairment level than the OP of the DF CR networks. There is a remarkable OP loss in the AF CR networks with almost 5 dB in SNDR when the impairment levels vary from 0.05 to 0.15; whereas the loss is about 1.5 dB in the DF CR networks. It can be explained by the fact that the AF protocol amplifies the distortion noises at S and accumulates the noises to the received signal at D, whereas the distortion noises from S are not amplified in the networks with DF relaying protocol.

Figure 2.3 illustrates the throughput of the CR networks with DF/AF relaying protocol under the impacts of transceiver impairments. It can be seen that both DF/AF CR networks can achieve similar maximum throughput in the high SNR (> 35 [dB]) region where the effect distortion noises caused by hardware impairments are much smaller than signal powers. However, in low SNR region, the networks with DF

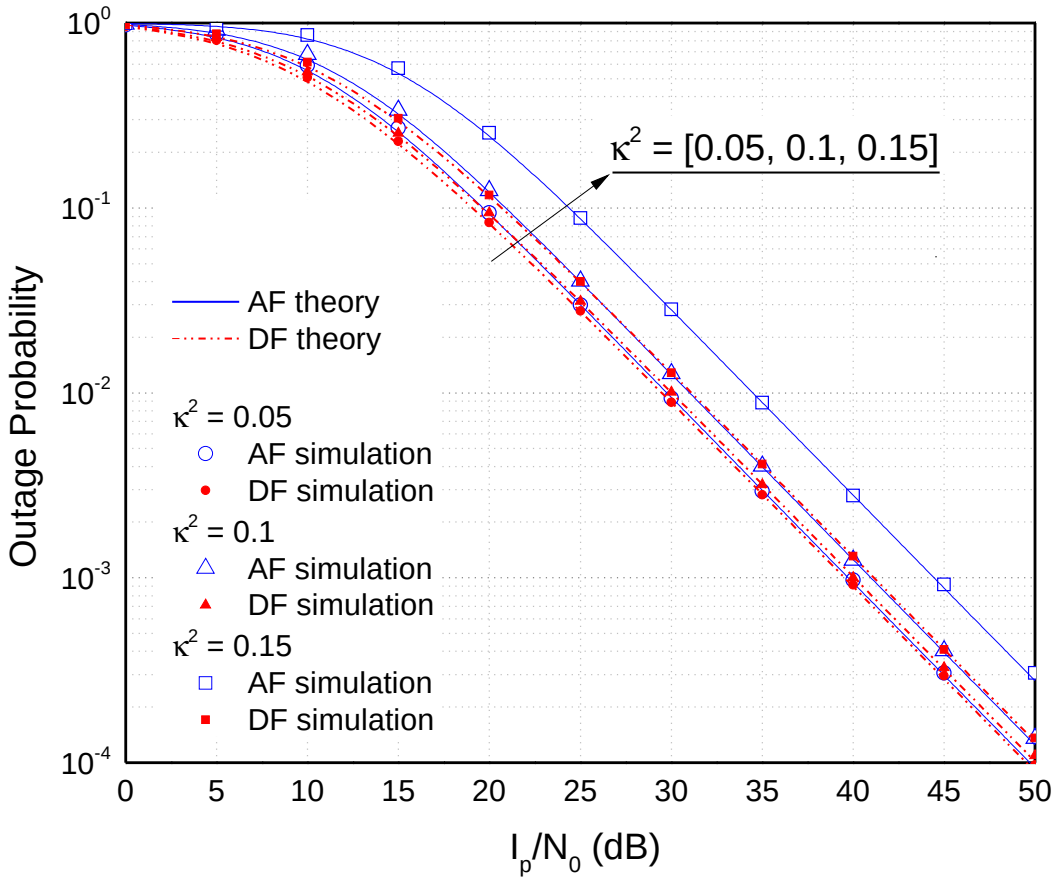

Figure 2.2: OP of the cognitive DF/AF relay networks

relaying protocol achieves better throughput than the one with AF relaying. This is because the DF CR networks has better OP than the AF CR networks. Interestingly, there are limiting values for the throughput of both DF CR networks and AF CR networks. The ceiling throughputs of the both relaying protocols are just under the fixed transmission rate of the source. In this specific simulation scenario, the ceiling throughput of the cognitive relay networks with DF or AF relaying protocol is 3.91[bits/sec/Hz].

2.6 Conclusion

We have analyzed the impact of the transceiver impairment on the OP and throughput of the DF/AF CR relay networks while the transmit powers are bounded by

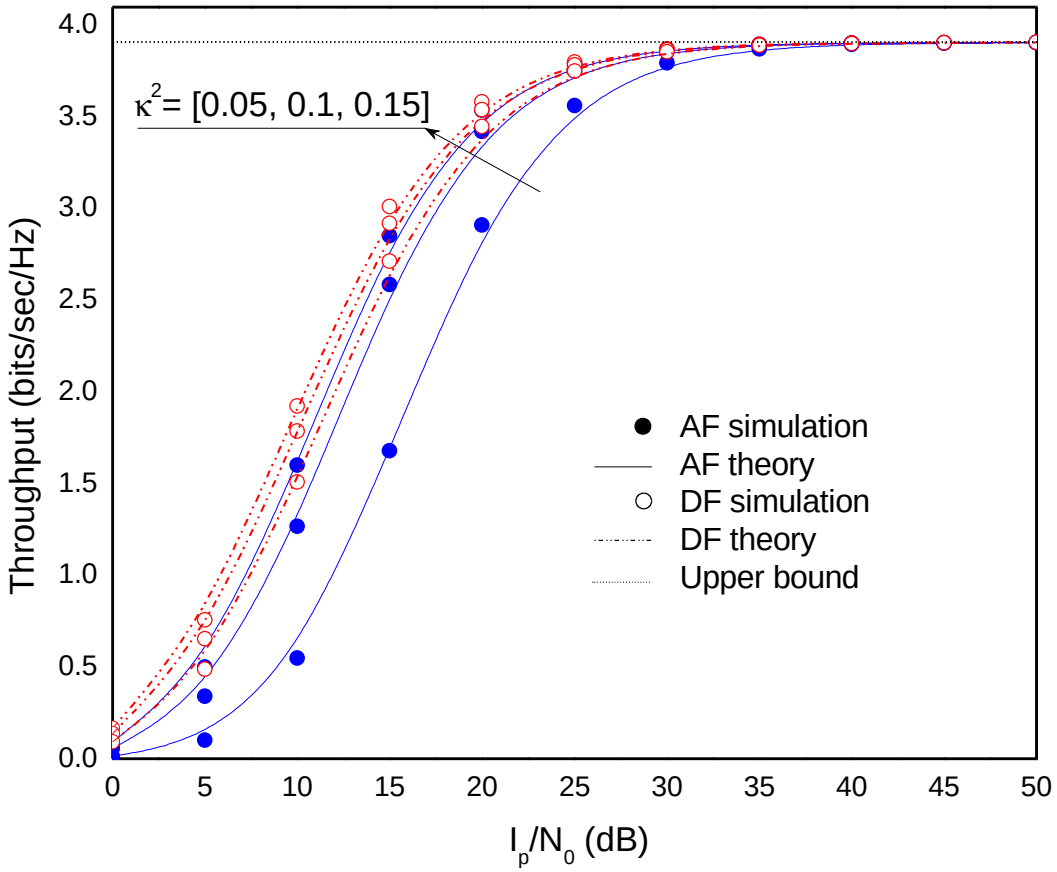

Figure 2.3: Throughput of the cognitive DF/AF relay networks

the maximum allowable transmit power parameter. The results confirm that the transceiver impairments deteriorates the performances of the networks. System performance degradation has been quantified as a function of the level of hardware impairments. Our analysis has provided engineering insights into the dual-hop CR relay networks: for instance, it was found that the DF CR networks outperforms the AF CR networks in both OP and throughput under the similar impacts of the transceiver impairments albeit at the expense of implementation complexity. In particular, the CR networks with DF protocol is less susceptible to transceiver impairments than the one with AF protocol. Ideally, these results can be used to determine the right relaying protocol for the CR networks with specific purpose and implementation cost. Furthermore, the analysis results can be directed the appropriate selection of transceiver hardware quality for the dual-hop CR networks in order to meet the predetermined OP and throughput.

3. Case study: Two-Way Cognitive Relay in RF Energy Harvesting Wireless Sensor Network

This chapter presents the exact outage performance and throughput of two-way cognitive decode-and-forward relaying wireless sensor networks with realistic transceiver relay. The relay is a self-powered wireless node that harvests radio frequency energy from the transmitted signals. We consider four configurations of a network with formed by combining two bidirectional relaying protocols (multiple access broadcast protocol and time division broadcast protocol), and two power transfer policies (dual-source energy transfer and single-fixed-source energy transfer). Based on our analysis, we provide practical insights into the impact of transceiver hardware impairments on the network performance, such as the fundamental capacity ceiling of the network with various configurations that cannot be exceeded by increasing transmit power given a fixed transmission rate and the transceiver selection strategy for the network nodes that can optimize the implementation cost and performance tradeoff.

3.1 Introduction

Cognitive radio has being discussed as a promising solution to combat the scarcity of frequency spectrum [5; 15; 28; 29]. In cognitive radio, secondary users are allowed to transmit wireless signals in the same frequency bands that are officially allocated to primary users. Hence, their the transmit powers are required to be

confined to the maximum allowable interference I_P that is defined by the primary receiver. In order to tackle the transmit power limitation in cognitive network, the concept of two-way cognitive relay (TWCR) networks [30–32] has been studied and is proved to be effective in improving the performance of cognitive relay network. It exploits the advantages of cognitive radio technology and the two-way relaying protocol to boost system performances.

The cognitive relay networking technique has recently become applicable to wireless sensor networks where the communication links between controller station and sensor nodes are assisted with low cost wireless-energy-harvesting relay nodes [33]. The intermediate relay node consumes its own power to process and forward the signal received from/to controller station to/from sensor nodes. This specific network is used for particular applications, such as wireless sensor networks in a forest where the power supply unit is difficult to recharge, hence a self-powered relay node is much preferred.

Relays are generally low-cost devices, therefore their transceiver hardware would produce several types of impairments such as, in-phase/quadrature imbalance [24; 25; 34], and high power amplifier nonlinearities [26]. However, most research contributions in the area of relay networking or cognitive relay networking have assumed that the relay node is perfect. In [30], a tight approximation of the outage probability of amplify-and-forward TWCR was provided. Closed-form expressions for the OP of a TWCR network in the presence of multiple primary users were derived in [31]. The relevant research on the OP and throughput of RF energy harvesting (EH) relay networks has also assumed perfect hardware (see [35; 36]).

Transceiver impairments unavoidably downgrade wireless system performances, especially in the system where low-cost wireless devices are employed. Motivated by the above discussion, in this work, we present a detailed performance analysis of an RF EH decode-and-forward (DF) TW cognitive relaying wireless sensor networks (WSNs) with imperfect transceiver hardware by utilizing the generalized impairment model of [13]. In particular, the contributions of this chapter are follows:

1. We portray a two-way DF cognitive relay wireless sensor network that can

be configured with four combinations of two transmission protocols and two energy transfer policies for RF self-powered DF TWCR networks.

2. Based on the network configuration, we provide new exact expressions for the OP and throughput in consider that the wireless transceiver of the network are modeled with hardware impairments model. We also tighten the constrain of transmit power limitation on the cognitive relay network to protect primary transmission link.

3. From our analysis, we put forward useful design guidelines for cognitive relay sensor network designers on selecting suitable transmission protocols and energy transfer policies for the network. Based on our analytical expressions, network designers can predict the impact of hardware impairments on the network performance hence, they can tolerate to achieve a predetermined outage probability and throughput.

4. We also suggest an effective hardware quality selection strategy that applied to controller station, relay nodes and sensor nodes. We could conclude that the network performance can be improved even with the low-cost relay node.

3.2 Network configuration and channel model

In this section, a case study of cognitive relay network is a wireless sensor network model with half-duplex two-way cognitive relaying protocol as illustrated in Fig. 3.1 is examined. In order to simplify the analysis, we consider a three-nodes cognitive relay network. The receiver (Rx) is the primary user; the secondary network consists of one controller station (node A), one sensor (node B) and one relay (node R). Each node is equipped with a single antenna. The controller station node A desires to transmit control data to the sensor node B and collect data from the sensor node. It is assumed that the light-of-sight wireless link between the controller station and the sensor is absent due to heavy shadowing and pathloss, whereas the links between Rx and each secondary node are available. Consequently, the relay R is utilized to assist the two-way transmission link. Furthermore, the necessary channel-state-information of all channels are supposed to be available at each node of the network.

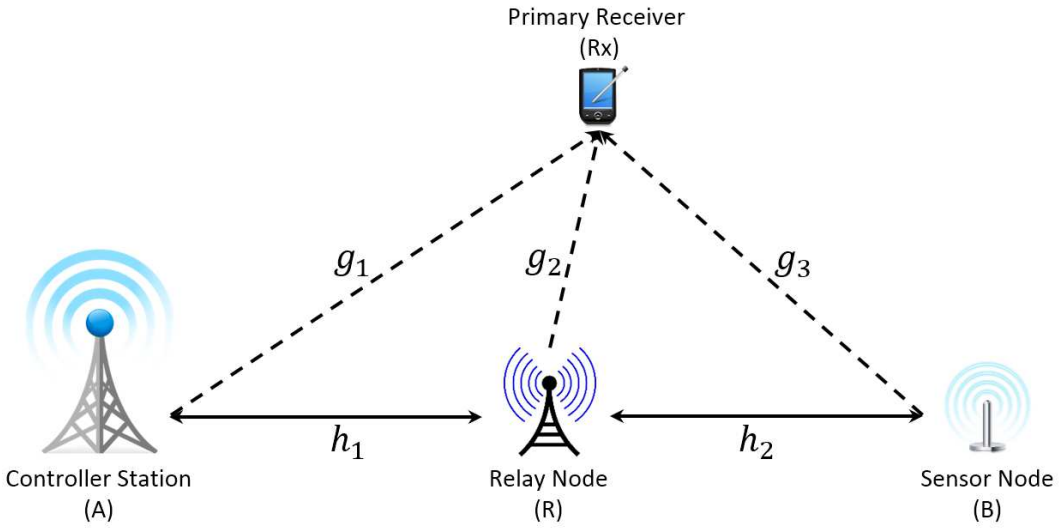

Figure 3.1: A Dual-hop half-duplex TWCR WSN.

All channels of the cognitive relay network are assumed to experience the quasi-static block Rayleigh fading whose coefficients are constant over the communication period T [36–39]. The channel coefficients of the wireless communication links $A \to R$, $R \to B$, $A \to Rx$, $B \to Rx$ and $R \to Rx$ are denoted as h_m and g_n where $m \in \{1,2\}$ and $n \in \{1,2,3\}$ and are complex Gaussian distributed with zero mean and variances $\frac{1}{\lambda_m}$, and $\frac{1}{\omega_n}$. The additive noise terms at A, B, and R are supposed to equal to η, where $\eta \sim \mathcal{CN}(0,N_0)$. The relay R harvests energy from RF signals before forward data to the designated destination. Since the transmit powers from A and B to the relay in the EH phase are independent from those in the information processing (IP) phase, we normalize the transmit powers in the former to unity, i.e. $P_A^{EH} = P_B^{EH} = 1$. We note that the normalized powers have to be equal or smaller than the maximum allowable transmit power.

In order to limit the effect of the interference powers from the secondary users to the primary receiver (Rx), the transmit powers in the IP phase of node A, B and R are limited by the maximum tolerance transmit power, I_P. Therefore, the maximum transmit powers at node A, B and R are $P_i = \frac{I_P}{|g_n|^2}$ where $i \in \{A,B,R\}$ and $n \in \{1,2,3\}$. For our analysis, we determine the exponentially distributed random variables $\rho_m = |h_m|^2$, and $\nu_n = |g_n|^2$ for $m \in \{1,2\}$ and $n \in \{1,2,3\}$, whose means are $\frac{1}{\lambda_m}$ and $\frac{1}{\omega_n}$, respectively. Finally, following the discussion in hardware impairment model section, the aggregate impairment levels during the IP phase at each secondary node are represented by κ_i^2 where $i \in \{A,B,R\}$. f_X and F_X are denoted

as the probability density function (PDF) and the cumulative distribution function (CDF) of random variable X. The CDF of X condition on random variable Y is described as $F_{X|Y}$.

3.3 Energy harvesting DF TWCR networks

We analyze a two-way cognitive relay network where the information exchanged from A to B is assisted by the intermediate relay node R that utilizes DF protocol. The ideal time switching-based relaying protocol with separated energy harvesting (EH) and information processing (IP) phases is applied at the relay [35]. In particular, the EH phase and IP phase switch over time in one communication period T. Relay harvests energy from transmitted wireless signals during αT [s] in the EH phase; whereas, desired transmit data are conveyed over $(1-\alpha)T$ [s] in the IP phase, where $0 < \alpha < 1$ is the time fraction parameter that determines the portion of EH phase and IP phase within one communication period T.

3.3.1 Energy harvesting phase

During the EH phase, the relay node harvests energy contained in the RF signals that are transmitted from the other nodes in the cognitive network. The collected energy is utilized to forward the signal from the relay to the desired destination. The amount of harvested energy depends on the time portion of the EH phase α and energy conversion efficiency μ. The energy conversion efficiency is determined by the rectification process and the EH circuit in the relay node, $0 < \mu \leq 1$ [37].Note that hardware impairments are not taken into account during the EH phase since: (a) the hardware used for harvesting energy is different from that used in transmitting/receiving data, and (b) any type of hardware imperfections in the EH circuitry is captured by μ. In this chapter, two transmitting energy policies are studied namely, dual-source (DS) energy transfer and signal-fixed-source (SFS) energy transfer.

3.3.1.1 Dual source energy transfer

Relay harvests energy from the signals that are transmitted from A and B in the cognitive DF network. The acquired energy at the relay node is parametrized as

$$E_H = \Upsilon \left(P_A^{EH} |h_1|^2 + P_B^{EH} |h_2|^2 \right) = \Upsilon(\rho_1 + \rho_2). \tag{3.1}$$

3.3.1.2 Single fixed source energy transfer

Relay harvests power from the signal that is transmitted from A or B which is predetermined before transmitting. Without loss of generality, the wireless signal for energy harvesting is assumed to be transmitted from node A. The energy harvested at the relay is given by

$$E_H = \Upsilon P_A^{EH} |h_1|^2 = \Upsilon \rho_1. \tag{3.2}$$

The energy conversion efficiency μ and the duration α of the energy harvesting phase affect the amount of the harvested energy in the EH phase.

In (3.1) and (3.2), Υ is an effective function that captures the effects of μ and α to the harvested energy E_H. The function Υ is specified for a given network configuration of the energy transfer policy in the EH phase and the relaying protocol in the IP phase. We describe two data transmission protocols of the IP phase in the next content.

3.3.2 Information processing phase

In this section, we discuss the information processing relaying protocols in the IP phase. We note that the IP phase occupies $(1-\alpha)$ portion of the T communication period.

3.3.2.1 Time division broadcast protocol

In TDBC protocol, the IP phase is divided into three time slots. In the first time slot, A broadcasts data to R. while B transmits data to R in the second time slot. The received data is decoded and re-encoded with a suitable network coding scheme, and then it is broadcasted to A and B in the third time slot. Assuming that the three time slots are similar in length, the TDBC is depicted in Fig. 3.2. The effective function is given by

$$\Upsilon_{tdbc} = \mu \frac{\alpha T}{(1-\alpha)T/3} = \frac{3\mu\alpha}{1-\alpha}. \tag{3.3}$$

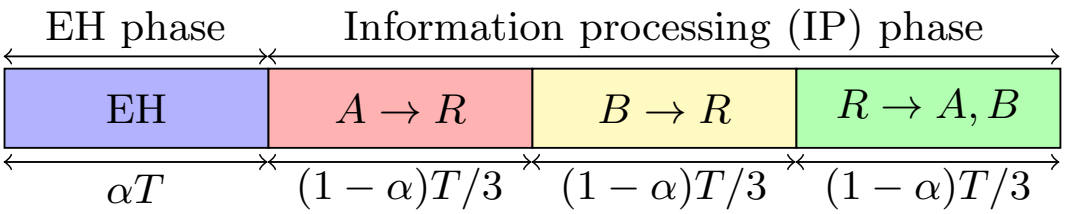

Figure 3.2: Data frame structure of TWRCN with TDBC protocol.

3.3.2.2 Multiple access broadcast protocol

In a multiple access broadcast (MABC) protocol, the IP phase is divided into two time slots. In the first time slot, R receives data from both node A and node B, while the received data is decoded and re-encoded with a suitable network coding scheme, then it is broadcasted to A and B in the second time slot. Assuming that the two time slots are similar in length, the TDBC is depicted in Fig. 3.3. The effective function is given by

$$\Upsilon_{mabc} = \mu \frac{\alpha T}{(1-\alpha)T/2} = \frac{2\mu\alpha}{1-\alpha}. \tag{3.4}$$

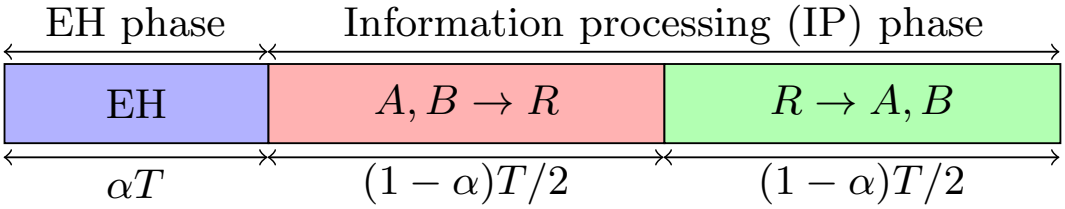

Figure 3.3: Data frame structure of TWRCN with MABC protocol.

3.4 Performance analysis

In this section, we elaborate on the signal-to-noise-plus-distortion ratio (SNDR) of the EH cognitive DF network for different energy transfer policies and relaying protocols by taking also into account the impact of transceiver impairments.

3.4.1 TDBC protocol with DS policy

In this subsection, it is assumed that the cognitive DF network utilizes the DS energy transfer policy in the EH phase and TDBC protocol in the IP phase. The harvested energy at R in the EH phase is given by substituting (3.3) into (3.1)

$$P_R = \Upsilon_{tdbc}(\rho_1 + \rho_2). \tag{3.5}$$

3.4.1.1 End-to-End SNDR

Since the information transfer from A and B to R are done in different time slots, the instantaneous SNDR at either R of the link $A \to R$ and $B \to R$ or at A (or at B) of the link $R \to A$ (or the link $R \to B$) respectively, are independent and statistically similar. Thus, without any loss of generality, only the link $A \to R \to B$ is investigated. Transmit power at A is $\frac{I_P}{|g_1|^2}$, then the SNDR at R of the link $A \to R$ is given by

$$\gamma_1 = \frac{\frac{I_P}{|g_1|^2}|h_1|^2}{\kappa_R^2 \frac{I_P}{|g_1|^2}|h_1|^2 + |\eta|^2} = \frac{\bar{\gamma}\rho_1}{\kappa_R^2 \bar{\gamma}\rho_1 + \nu_1}. \tag{3.6}$$

where κ_R^2 is the aggregate impairment level of the $A \to R$ link, while $\bar{\gamma} = \frac{I_P}{N_0}$. The received signals are forwarded to A and B in the third time slot of the TDBC protocol. Transmit power at R in the IP phase is $\frac{P_R}{|g_2|^2}$ where P_R is given in (3.5), then the SNDR at B of the link $R \to B$ is given by

$$\gamma_2 = \frac{\frac{P_R}{|g_2|^2}|h_2|^2}{\kappa_B^2 \frac{P_R}{|g_2|^2}|h_2|^2 + |\eta|^2} = \frac{\Upsilon_{tdbc}\bar{\gamma}(\rho_1+\rho_2)}{\kappa_B^2 \Upsilon_{tdbc}\bar{\gamma}(\rho_1+\rho_2)+\frac{v_2}{\rho_2}}. \tag{3.7}$$

The end-to-end SNDR of the cognitive DF network is then given as

$$\gamma = \min(\gamma_1, \gamma_2). \tag{3.8}$$

3.4.1.2 Outage performance analysis

Based on (3.8), the CDF of γ, $F_\gamma(\gamma)$, is mathematically evaluated as

$$F_\gamma(\gamma) = F_{\gamma_1}(\gamma) + F_{\gamma_2}(\gamma) - F_{\gamma_1}(\gamma)F_{\gamma_2}(\gamma). \tag{3.9}$$

Note that ρ_1 appears as a common random variable in both γ_1 and γ_2. Hence, the CDF of γ needs to be manipulated with the help of conditional and total probability laws. The CDF of γ is obtained as

$$F_\gamma(\gamma) = \int_0^\infty \left[F_{\gamma_1|\rho_1}(\gamma) + F_{\gamma_2|\rho_1}(\gamma) - F_{\gamma_1|\rho_1}(\gamma)F_{\gamma_2|\rho_1}(\gamma)\right] f_{\rho_1}(x)dx. \tag{3.10}$$

The following theorems will enable us to evaluate (3.10).

Theorem 3.1. *The CDF of γ_1 conditioned on ρ_1, $F_{\gamma_1|\rho_1}$, is given by*

$$F_{\gamma_1|\rho_1}(\gamma) = \exp\left(-\frac{\bar{\gamma}(1-\kappa_R^2\gamma)}{\omega_1\gamma}\rho_1\right). \tag{3.11}$$

Proof. From the definition of the CDF we have

$$\begin{aligned} F_{\gamma_1|\rho_1}(\gamma) &= \Pr\left[\frac{\bar{\gamma}\rho_1}{\kappa_R^2\bar{\gamma}\rho_1+\nu_1} \le \gamma\right] \\ &= \Pr\left[\nu_1 \ge \frac{\bar{\gamma}(1-\kappa_R^2\gamma)\rho_1}{\gamma}\right] \\ &= 1 - F_{\nu_1}\left(\frac{\bar{\gamma}(1-\kappa_R^2\gamma)\rho_1}{\gamma}\right). \end{aligned}$$

This result leads directly to (3.11). □

Theorem 3.2. *The CDF of γ_2 conditioned on ρ_1, $F_{\gamma_2|\rho_1}$, is given by*

$$F_{\gamma_2|\rho_1}(\gamma) = \frac{\omega_2}{\lambda_2^2 C_1}\exp\left(\frac{\rho_1}{\lambda_2}\right)\exp\left(\frac{\omega_2}{\lambda_2^2 C_1}\right)E_1\left(\frac{\omega_2}{\lambda_2^2 C_1}\right). \tag{3.12}$$

where $C_1 \triangleq \frac{\Upsilon_{tdbc}\bar{\gamma}(1-\kappa_B^2\gamma)}{\gamma}$, and $E_1(x) = \int_x^\infty \frac{e^{-t}}{t}dt$ is the exponential integral function.

Proof. By the definition of CDF, we have

$$\begin{aligned} F_{\gamma_2|\rho_1}(\gamma) &= \Pr\left[\frac{\Upsilon_{tdbc}\bar{\gamma}(\rho_1+\rho_2)}{\kappa_B^2\Upsilon_{tdbc}\bar{\gamma}(\rho_1+\rho_2)+\frac{\nu_2}{\rho_2}} \le \gamma\right] \\ &= 1 - \Pr\left[\frac{\nu_2}{\rho_2} \le C_1(\rho_1+\rho_2)\right] \\ &= 1 - \int_0^\infty F_X(C_1 y)\, f_{Y|\rho_1}(y)dy. \end{aligned} \tag{3.13}$$

where $X \triangleq \frac{\nu_2}{\rho_2}$ and $Y \triangleq \rho_1+\rho_2$. It is apparent that $F_X(x) = 1 - \frac{\omega_2}{x\lambda_2+\omega_2}$ and $f_{Y|\rho_1}(y) = \frac{1}{\lambda_2}\exp\left(-\frac{y-\rho_1}{\lambda_2}\right)$. Substituting these results into (3.13), we obtain

$$F_{\gamma_2|\rho_1}(\gamma) = \int_0^\infty \left(\frac{\omega_2}{\omega_2+\lambda_2 y}\right)\frac{1}{\lambda_2}\exp\left(-\frac{y-\rho_1}{\lambda_2}\right)dy. \tag{3.14}$$

After some algebra manipulations and using [40, Eq. (3.352.4)], we obtain the result as shown in (3.12). □

Now, (3.10) can be re-expressed as

$$F_\gamma(\gamma) = I_1 + I_2 - I_3. \tag{3.15}$$

where we can define from Theorem 3.1 and Theorem 3.2:

$$\begin{aligned}
I_1 &= \frac{\omega_1 \gamma}{\omega_1 \gamma + \lambda_1 \bar{\gamma}(1-\kappa_R^2 \gamma)}, \\
I_2 &= C_2 \frac{\lambda_2}{\lambda_1+\lambda_2}, C_2 \triangleq \frac{\omega_2}{\lambda_2^2 C_1} \exp\left(\frac{\omega_2}{\lambda_2^2 C_1}\right) \mathrm{E}_1\left(\frac{\omega_2}{\lambda_2^2 C_1}\right), \\
I_3 &= C_2 \frac{\lambda_2 \omega_1}{\lambda_1 \lambda_2 \bar{\gamma}(1-\kappa_R^2 \gamma) + \omega_1 \gamma(\lambda_1+\lambda_2)}.
\end{aligned}$$

Finally, the OP at nodes A and B under a specified SNDR threshold (γ_t) of the network are given in (3.16) and (3.17).

$$\begin{aligned}
OP_A(\gamma_t) =& \frac{\omega_3 \gamma_t}{\omega_3 \gamma_t + \lambda_2 \bar{\gamma}(1-\kappa_R^2 \gamma_t)} + \frac{\omega_2}{\lambda_1^2 C_1} \exp\left(\frac{\omega_2}{\lambda_1^2 C_1}\right) \mathrm{E}_1\left(\frac{\omega_2}{\lambda_1^2 C_1}\right) \\
&\times \left[\frac{\lambda_1}{\lambda_2+\lambda_1} - \frac{\lambda_1 \omega_3}{\lambda_2 \lambda_1 \bar{\gamma}(1-\kappa_R^2 \gamma_t) + \omega_3 \gamma_t (\lambda_2+\lambda_1)}\right].
\end{aligned} \tag{3.16}$$

$$\begin{aligned}
OP_B(\gamma_t) =& \frac{\omega_1 \gamma_t}{\omega_1 \gamma_t + \lambda_1 \bar{\gamma}(1-\kappa_R^2 \gamma_t)} + \frac{\omega_2}{\lambda_2^2 C_1} \exp\left(\frac{\omega_2}{\lambda_2^2 C_1}\right) \mathrm{E}_1\left(\frac{\omega_2}{\lambda_2^2 C_1}\right) \\
&\times \left[\frac{\lambda_2}{\lambda_1+\lambda_2} - \frac{\lambda_2 \omega_1}{\lambda_1 \lambda_2 \bar{\gamma}(1-\kappa_R^2 \gamma_t) + \omega_1 \gamma_t (\lambda_1+\lambda_2)}\right].
\end{aligned} \tag{3.17}$$

3.4.1.3 Throughput analysis

In this part, we analyze the network throughput in the context of delay-limited transmission. We assume that the sources transmit information to destinations at a fixed communication rate. The transmission rates at A and B of the TWCR networks are given as $R_A = \log_2(1+\gamma_A)$ and $R_B = \log_2(1+\gamma_B)$ [bit/sec/Hz], respectively, where γ_A and γ_B are threshold SNDRs. The network throughput is measured as the sum of throughput of each transmission link that is sufficient for transmitting at the given rate. Hence, the network throughput, $\mathcal{T}$, in the TDBC protocol is determined as

$$\mathcal{T} = \frac{(1-\alpha)}{3} \left[R_A(1-OP_A(\gamma_A)) + R_B(1-OP_B(\gamma_B))\right]. \tag{3.18}$$

where $OP_A(\gamma_A)$ and $OP_B(\gamma_B)$ is the outage probability at A and B respectively. The network throughput in this case is obtained by substituting the outage probability at A and B from (3.17) and (3.18).

3.4.2 TDBC protocol with SFS policy

In this subsection, we consider the cognitive DF network operating with the SFS energy transfer policy in the EH phase and TDBC protocol in the IP phase. The harvested energy at R in the EH phase is given by substituting 3.3 into (3.2)

$$P_R = \Upsilon_{tdbc}\rho_1. \tag{3.19}$$

3.4.2.1 End-to-End SNDR

Since the transmit power at R is harvested from A, the SNDR of the $A \to R \to B$ link is different from the SNDR of the $B \to R \to A$. First, we analyze the $A \to R \to B$ link. Transmit power at A equals $\frac{I_P}{|g_1|^2}$; whereas transmit power at R is $\frac{P_R}{|g_2|^2}$, P_R is given in (3.19). Hence, the SNDRs at R and B given respectively by

$$\gamma_{1,ARB} = \frac{\frac{I_P}{|g_1|^2}|h_1|^2}{\kappa_R^2\frac{I_P}{|g_1|^2}|h_1|^2 + |\eta|^2} = \frac{\bar{\gamma}\rho_1}{\kappa_R^2\bar{\gamma}\rho_1 + \nu_1}. \tag{3.20}$$

$$\gamma_{2,ARB} = \frac{\frac{P_R}{|g_2|^2}|h_2|^2}{\kappa_B^2\frac{P_R}{|g_2|^2}|h_2|^2 + |\eta|^2} = \frac{\Upsilon_{tdbc}\bar{\gamma}\rho_1\rho_2}{\kappa_B^2\Upsilon_{tdbc}\bar{\gamma}\rho_1\rho_2 + \nu_2}. \tag{3.21}$$

Thus, the end-to-end SNDR at B is given by

$$\gamma_B = \min(\gamma_{1,ARB}, \gamma_{2,ARB}). \tag{3.22}$$

Consider the $B \to R \to A$ link, transmit power at B equals $\frac{I_P}{|g_3|^2}$; whereas transmit power at R is $\frac{P_R}{|g_2|^2}$, P_R is given in (3.19). Therefore, the SNDRs at R and A are

respectively given by

$$\gamma_{1,BRA} = \frac{\frac{I_P}{|g_3|^2}|h_2|^2}{\kappa_R^2 \frac{I_P}{|g_3|^2}|h_2|^2 + |\eta|^2} = \frac{\bar{\gamma}\rho_2}{\kappa_R^2 \bar{\gamma}\rho_2 + \nu_3}. \tag{3.23}$$

$$\gamma_{2,BRA} = \frac{\frac{P_R}{|g_2|^2}|h_1|^2}{\kappa_A^2 \frac{P_R}{|g_2|^2}|h_1|^2 + |\eta|^2} = \frac{\Upsilon_{tdbc}\bar{\gamma}\rho_1}{\kappa_A^2 \Upsilon_{tdbc}\bar{\gamma}\rho_1 + \frac{\nu_2}{\rho_1}}. \tag{3.24}$$

The end-to-end SNDR at A is given by

$$\gamma_A = \min(\gamma_{1,BRA}, \gamma_{2,BRA}). \tag{3.25}$$

3.4.2.2 Outage performance analysis

It can be seen that the random variable ρ_1 appears as a common random variable in both $\gamma_{1,ARB}$ and $\gamma_{2,ARB}$. Hence, the end-to-end CDF γ_{ARB} needs to be manipulated with the help of conditional and total probability laws as before:

$$\begin{aligned} F_{\gamma_B}(\gamma) = \int_0^\infty \big[& F_{\gamma_{1,ARB}|\rho_1}(\gamma) + F_{\gamma_{2,ARB}|\rho_1}(\gamma) \\ & - F_{\gamma_{1,ARB}|\rho_1}(\gamma) F_{\gamma_{,ARB}|\rho_1}(\gamma) \big] f_{\rho_1}(x) dx. \end{aligned} \tag{3.26}$$

Theorem 3.3. *The CDF of $\gamma_{2,ARB}$ conditioned on ρ_1, $F_{\gamma_{2,ARB}|\rho_1}$, is given by*

$$F_{\gamma_{2,ARB}|\rho_1}(\gamma) = \frac{\omega_2 \gamma}{\omega_2 \gamma + (1 - k_B^2 \gamma)\bar{\gamma}\Upsilon_{tdbc}\lambda_2 \rho_1}. \tag{3.27}$$

Proof. From the definition of the CDF, we have

$$\begin{aligned} F_{\gamma_{2,ARB}|\rho_1}(\gamma) &= \Pr\left[\frac{\Upsilon_{tdbc}\bar{\gamma}\rho_1\rho_2}{\kappa_B^2 \Upsilon_{tdbc}\bar{\gamma}\rho_1\rho_2 + \nu_2} < \gamma \right] \\ &= 1 - \int_0^\infty F_{\nu_2}\left(\frac{\Upsilon_{tdbc}\bar{\gamma}(1 - \kappa_B^2\gamma)\rho_1 x}{\gamma} \right) f_{\rho_2}(x) dx. \end{aligned}$$

By substituting the CDF and PDF of the exponential random variable ρ_2 to the above equation, $F_{\gamma_{2,ARB}|\rho_1}$ can be obtained as in (3.27). □

The CDF of $\gamma_{1,ARB}$ conditioned on ρ_1 can be obtained via Theorem 3.1, while the CDF of $\gamma_{2,ARB}$ conditioned on ρ_1 is deduced through Theorem 3.3. For instance, we can readily show that

$$F_{\gamma_{1,ARB}|\rho_1}(\gamma) = \exp\left(-\frac{\bar{\gamma}(1-\kappa_R^2\gamma)\rho_1}{\omega_1\gamma}\right). \tag{3.28}$$

Thus, the end-to-end CDF of γ_B is derived by substituting all previous results to (3.26).

$$\begin{aligned} F_{\gamma_B}(\gamma) =& \frac{1}{\lambda_1 C_3} + \frac{1}{\lambda_1 C_1}\exp\left(\frac{1}{\lambda_1 C_1}\right)\mathrm{E}_1\left(\frac{1}{\lambda_1 C_1}\right) \\ &\times \frac{1}{\lambda_1 C_1}\exp\left(\frac{C_3}{\lambda_1 C_1}\right)\mathrm{E}_1\left(\frac{C_3}{\lambda_1 C_1}\right). \end{aligned} \tag{3.29}$$

where $C_3 \triangleq \frac{\bar{\gamma}\lambda_1(1-\kappa_R^2\gamma)+\omega_1\gamma}{\lambda_1\omega_1\gamma}$.

We now turn our attention to $F_{\gamma_A}(\gamma)$. We first note that $\gamma_{1,BRA}$ and $\gamma_{2,BRA}$ are mutually independent random variables as shown in (3.23). Thus, the CDF of γ_A can be expressed as

$$F_{\gamma_A}(\gamma) = F_{\gamma_{1,BRA}}(\gamma) + F_{\gamma_{2,BRA}}(\gamma) - F_{\gamma_{1,BRA}}(\gamma)F_{\gamma_{2,BRA}}(\gamma). \tag{3.30}$$

The CDF of $\gamma_{1,BRA}$ is found based on Theorem 3.3, while the CDF of $\gamma_{2,BRA}$ is derived with the help of Theorem 3.2. In particular, we have that

$$F_{\gamma_{1,BRA}}(\gamma) = \frac{\gamma\omega_3}{\gamma\omega_3 + \bar{\gamma}\lambda_2(1-\kappa_R^2\gamma)}. \tag{3.31}$$

$$F_{\gamma_{2,BRA}}(\gamma) = \frac{\omega_2}{\lambda_1^2 C_4}\exp\left(\frac{\omega_2}{\lambda_1^2 C_4}\right)\mathrm{E}_1\left(\frac{\omega_2}{\lambda_1^2 C_4}\right). \tag{3.32}$$

where $C_4 \triangleq \frac{\Upsilon_{tdbc}\bar{\gamma}(1-\kappa_A^2\gamma)}{\gamma}$. Combining all the previous results together, the outage probabilities at A and B under the specified SNDR threshold (γ_t) of the network are

given in (3.33)–(3.34).

$$OP_A(\gamma_t) = \frac{\gamma_t \omega_3}{\gamma_t \omega_3 + \bar{\gamma}\lambda_2(1-\kappa_R^2\gamma_t)} + \frac{\omega_2}{\lambda_1^2 C_4} \exp\left(\frac{\omega_2}{\lambda_1^2 C_4}\right) \mathrm{E}_1\left(\frac{\omega_2}{\lambda_1^2 C_4}\right) \left[1 - \frac{\gamma_t \omega_3}{\gamma_t \omega_3 + \bar{\gamma}\lambda_2(1-\kappa_R^2\gamma_t)}\right]. \quad (3.33)$$

$$OP_B(\gamma_t) = \frac{1}{\lambda_1 C_3} + \frac{1}{\lambda_1 C_1} \exp\left(\frac{1}{\lambda_1 C_1}\right) \mathrm{E}_1\left(\frac{1}{\lambda_1 C_1}\right) \frac{1}{\lambda_1 C_1} \exp\left(\frac{C_3}{\lambda_1 C_1}\right) \mathrm{E}_1\left(\frac{C_3}{\lambda_1 C_1}\right). \quad (3.34)$$

3.4.2.3 Throughput analysis

As in Section 3.4.1.3, the network throughput with delay limited transmission is obtained as (3.18) in which $OP_A(\gamma_A)$ and $OP_B(\gamma_B)$ denote the outage probability at A and B obtained from (3.33) and (3.34).

3.4.3 MABC protocol with DS and SFS policy

As the direct communication link between A and B is not considered in our analysis, the SNDRs at A and B in the MABC protocol are similar to the SNDRs in TDBC protocol. However, the effective function Υ is different between the two protocols as indicated in (3.3) and (3.4). Therefore, the OP and throughput of the MABC protocol can be evaluated by following a similar line of reasoning as for the TDBC protocol, with the only difference pertaining to the replacement of Υ_{tdbc} with Υ_{mabc}.

3.5 Simulation and analysis

In this section, the outage probability and throughput of our analysis are evaluated using Monte Carlo simulation. The analytical results of outage probability are calculated using the equations from our analysis in Section 3.3, whereas the simulation results are obtained by Monte-Carlo simulation method similar to [29], [32] and [35].

Analytical results: In order to calculate the analytical results, the fading of the wireless channels are characterized by Rayleigh distribution of which the means are zero and the variances equal to the path loss. We calculate the outage probability of the network by plunging the fading channel' variances and the simulation parameters in Table **??** into the analysis equations (3.16), (3.17) for the network with DS energy transfer policy and (3.33), (3.34) for the network with SFS policy.

Simulation results: In the Monte Carlo simulation, the fading channels, that are characterized by Rayleigh distribution with zero mean and variance as the path loss, are generated randomly in *Matlab*. We imitate the actual data transmission in the network with that random fading channel in order to evaluate the simulation outage probability. 50 data frames are transmitted from the controller station A to the sensor node B via the relay node R. Each frame consists of 2^{13} bits. The network are configured with MABC/TDBC relaying protocol and DS/SFS energy transfer policy.

Then, the analytical and simulation results of throughput are obtained by plugging the analytical and simulation results of outage probability into (3.18), respectively.

For the sake of validation, all the wireless channels in the network are assumed to be affected by path loss and Rayleigh fading. The path loss is model as deterministic process d^{-2}, where d is the transmit distance. Whereas, the channel fading agreed with Rayleigh distribution.

Unless otherwise stated, we consider a network with equal transmission rate at A and B are $R_A = R_B = 2$ [bits/sec/Hz], respectively. Hence, the outage threshold is $\gamma_t = 2^2 - 1 = 3$. Transceivers in the network are hardware impairment model. The impairment levels are examined in the range $[0.08, 0.175]$, of which resembles the requirements of error vector magnitudes (EVMs) of 3GPP LTE. The duration of EH and IP phase in both TDBC and MABC protocol are assumed to be taken two ratios, $\alpha = [0.2, 0.5]$. The energy conversion efficiency is set to $\mu = 0.8$. The simulation parameters of the network are given in Table 3.1.

Furthermore, the network is placed in a 2-D Cartesian of which the controller station A is located at the origin. The nodes R, B and Rx are placed in the plan where the coordinates are $(0.4;0)$, $(1;0)$ and $(0.8;0.8)$ respectively. Based on the network

topology, we can calculate the transmit distance d of every transmission link, for instance transmit distance from A to R is $d_{A,R} = 0.4$. $\bar{\gamma}$ is the average SNDR.

Table 3.1: Simulation parameters for the two-way cognitive relay network

Name	**Value**
Fading model	Rayleigh
Path loss model	Exponential d^{-2}
Frame size	2^{13} [bits]
Number of frame	50 [frames]
Transmission rate	$R_A = R_B = 2$ [bits/sec/Hz]
Outage threshold	$\gamma_t = 3$
Hardware impairment level	$\kappa_A^2, \kappa_B^2, \kappa_R^2 \in [0.08; 0.175]$
Timing ratio of EH/IP phase	$\alpha = [0.2; 0.5]$
Energy conversion efficiency	$\mu = 0.8$

3.5.1 Outage probability result

Fig. 3.4–3.6 show the OP of the two-way cognitive DF relaying network under different hardware impairment levels for various network configurations. The analytical results of OP were obtain from Eq. (18), (3.17), (3.33), and (3.34). It can be seen that the analysis and simulation results are identical in all cases. As anticipated, the OP at A and B in the DS energy transfer policy are similar while they differ in the SFS policy; OP is higher for the TDBC transmission protocol than for the MABC protocol. This is because the latter scheme requires only two time slots to forward data to the destination, whilst the latter needs three time slots to do so. In addition, the impact of transceiver imperfections is dramatically enlarged with an increase of the hardware impairment levels. More specifically, we experience a 1.5 [dB] loss in the signal-to-noise ratio in order to maintain the OP at nodes A and B when the impairment level κ^2 increases from 0.08 to 0.175. In addition, we found that the OP at A in the SFS energy transfer policy is lower compared to the OP at B in the SFS policy and A and B in the DS policy. The impact of hardware impairment on OP is similar for TDBC or MABC protocol, however the network utilizing DS policy is more sensitive to transceiver impairment than SFS policy.

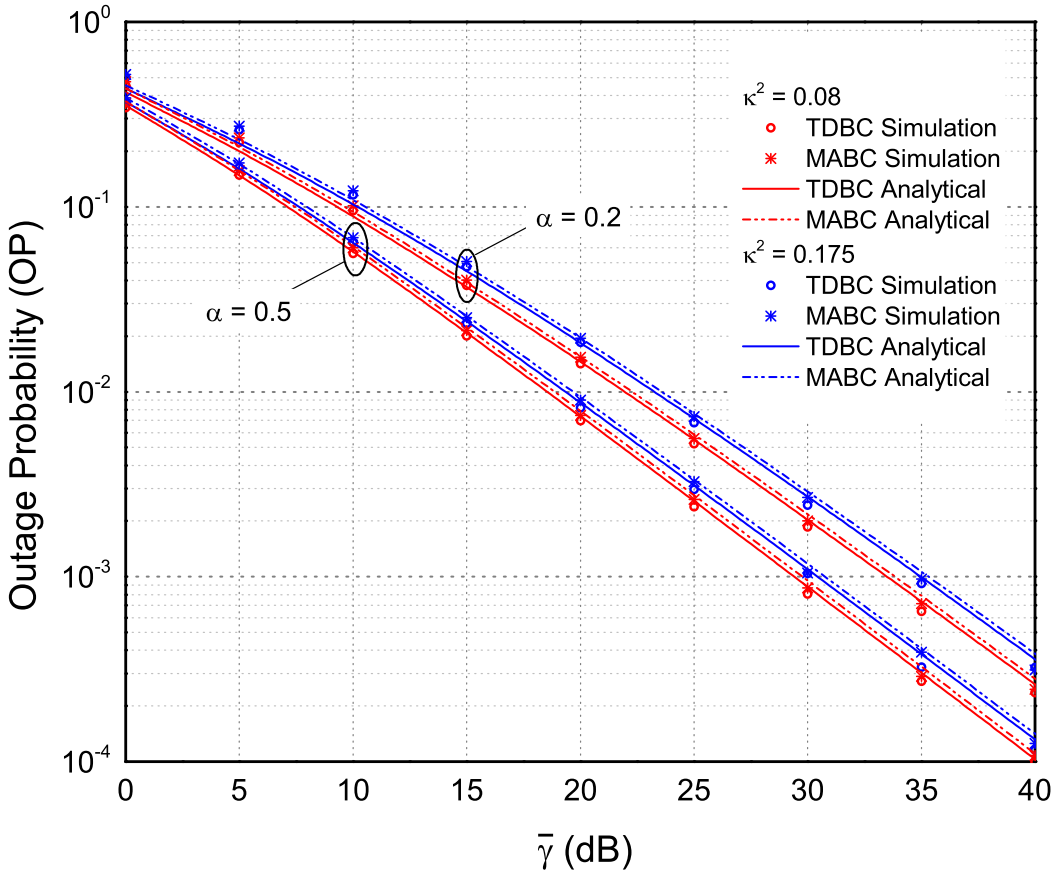

Figure 3.4: OP of TDBC and MABC protocol with DS policy.

3.5.2 Fundamental ceiling throughput

Fig. 3.7 illustrates the throughput of the two-way cognitive DF relay network under different hardware impairment levels in various transmission protocols and power transfer policies. The analytical results of network throughput were obtain from Eq. (3.18) by plugging (3.16), (3.17), (3.33), and (3.34). It can be seen that the throughput of the MABC protocol outperforms that of the TDBC protocol, while DS energy transfer policy provides better throughout than SFS policy. In fact, the throughput of MABC protocol combined with DS energy transfer is highest among the four combinations; on the other end, TDBC with SFS energy transfer provides the smallest throughput. This phenomenon can be attributed to the fact that the transmission time in MABC protocol is more efficiently utilized than in the TDBC protocol; however, MABC protocol is more sophisticated in implementation since the relay receives signals from A and B in the one time slot. Note also that DS

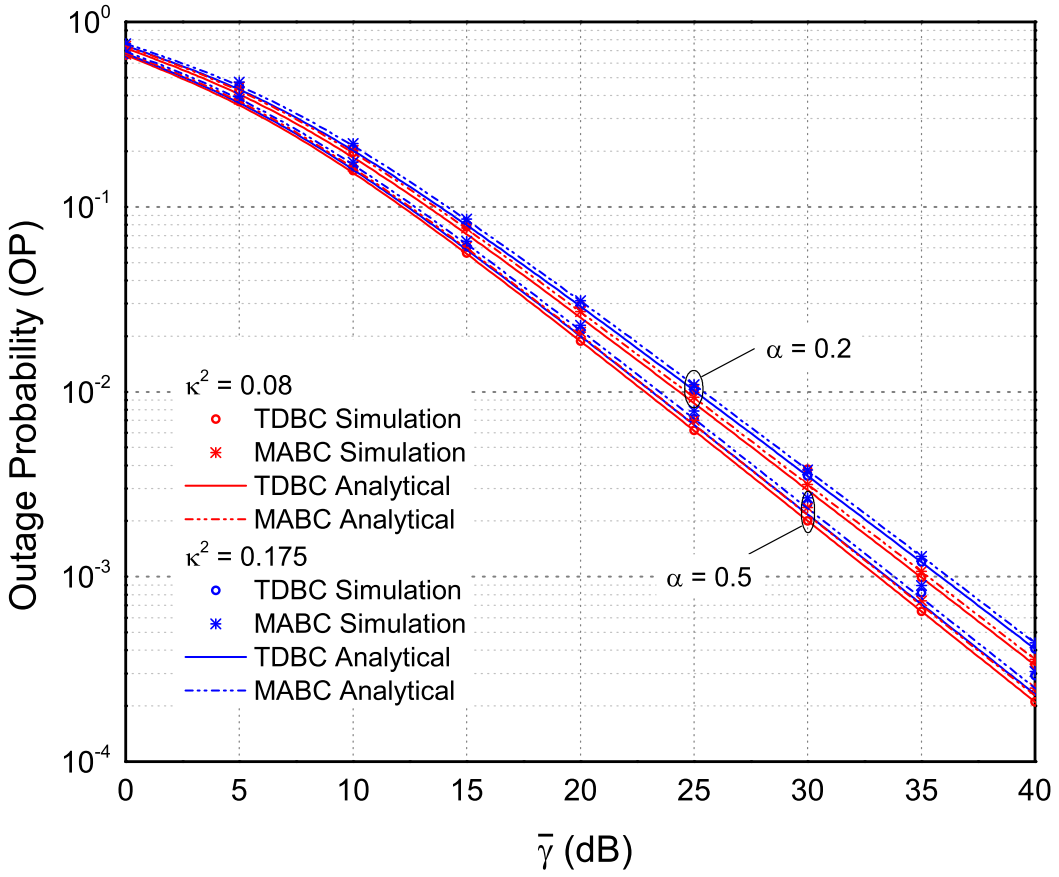

Figure 3.5: OP at A of TDBC and MABC protocol with SFS policy.

energy transfer offers higher throughput since the relay can harvests more power than compared to the SFS policy. Interestingly, there are limiting values for the throughput of both MABC and TDBC information transmission protocols. The highest throughput of the MABC protocol almost equals that of the fixed transmission rate of the sources, while the ceiling throughput of the TBDC protocol is lower than the rate. In our scenario with transmission rate $R_A = R_B = 2$ [bits/sec/Hz], the ceiling throughput of the MABC and TDBC protocols with $\alpha = 0.2$ are 1.6 and 1 [bits/sec/Hz], respectively; whilst, 1.07 and 0.67 [bits/sec/Hz], respectively with $\alpha = 0.5$.

We found that the impact of transceiver hardware impairments on throughput of the network with four configurations is remarkable in the low SNR regime ($\frac{I_P}{N_0} < 10$ dB). However, this effect is fair in the higher SNR ($10 < \frac{I_P}{N_0} < 15$ dB) regime and disappear in the high SNR region ($\frac{I_P}{N_0} > 20$ dB) when the maximum throughput is

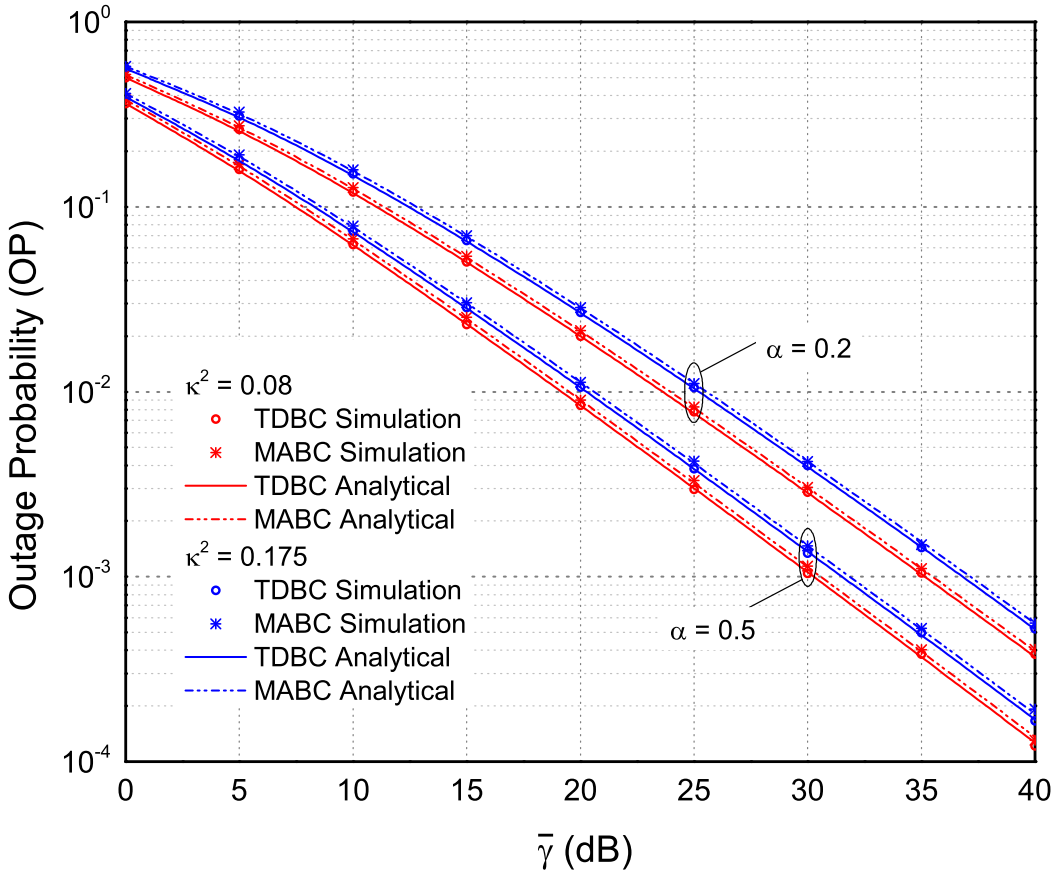

Figure 3.6: OP at B of TDBC and MABC protocol with SFS policy.

established. Specifically, the impact of hardware impairments on throughput of the network with MABC protocol is higher than that in the TDBC network. Furthermore, the network throughput decreases as α increases. The effect of the factor α to the throughput can be explained by (3.18). In case of the EH duration is much longer than the IP duration, $\alpha \gg 0$, the achieved throughput is approaching to zero. Therefore, the suitable selection value of α is important to achieve high performance.

3.5.3 Hardware quality selection strategy

Fig. 3.8–Fig. 3.11 illustrates the detail impact of transceiver impairments at A, B and R on network throughput. We observe a scenario where the channel condition is not so good ($SNDR = 5dB$); the duration ratio of the EH and IP phase is $\alpha = 0.5$; the

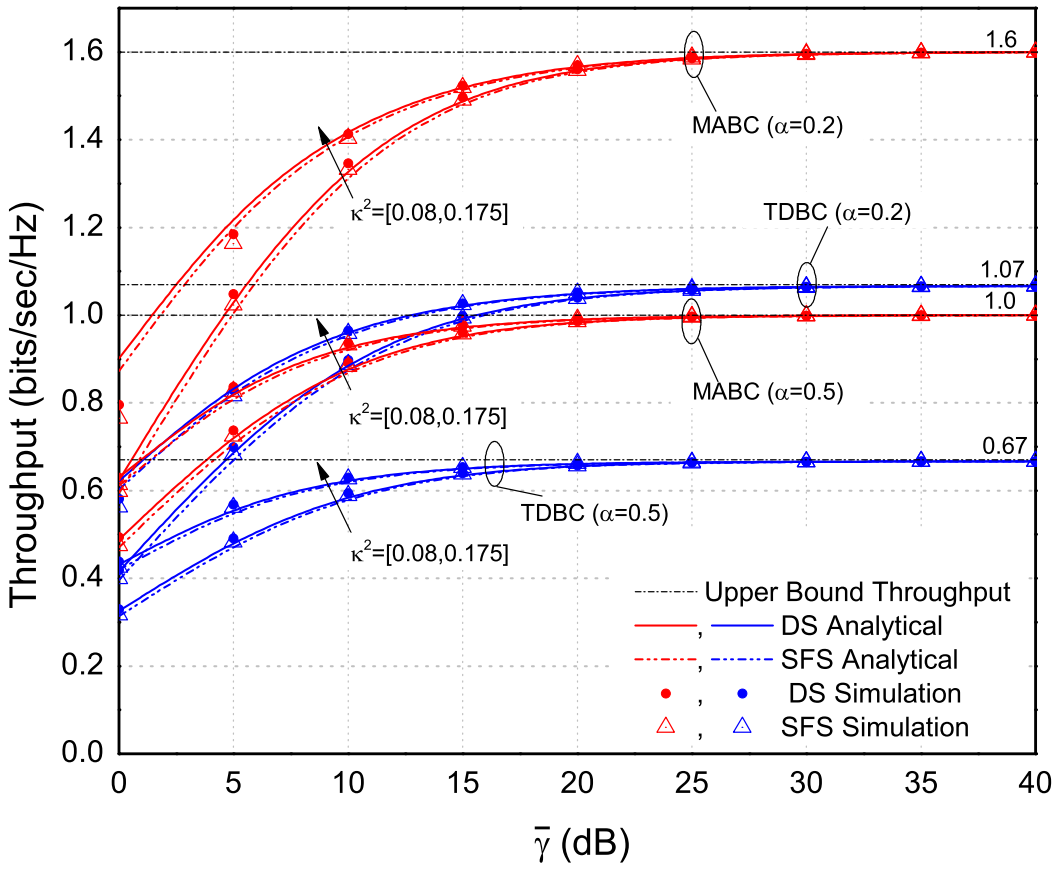

Figure 3.7: Network throughput for TDBC and MABC protocol with different energy transfer policies.

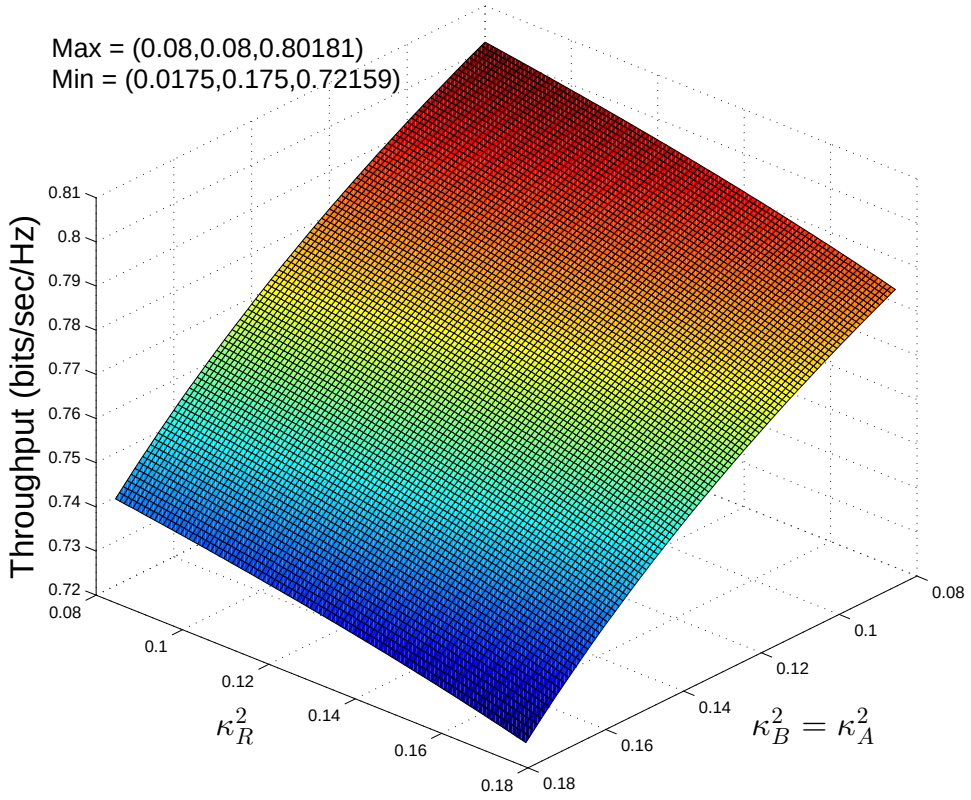

Figure 3.8: The detail impact of hardware impairment at A, B and R on network throughput when $SNDR = 5dB$ with MABC protocol and DS policy

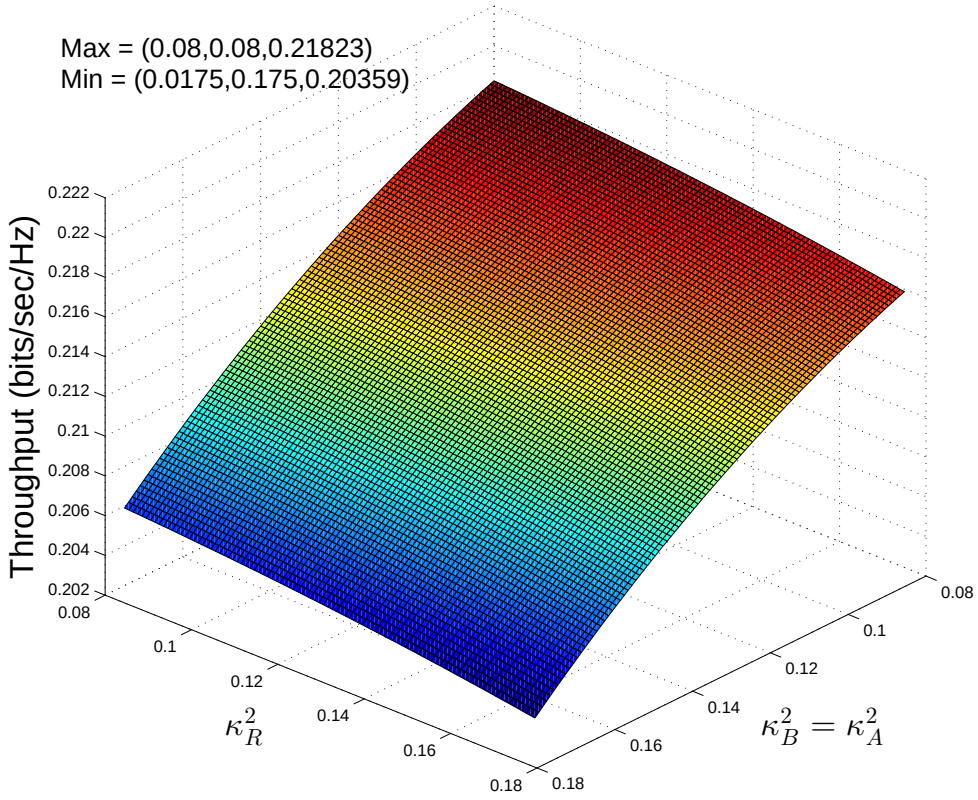

Figure 3.9: The detail impact of hardware impairment at A, B and R on network throughput when $SNDR = 5dB$ with MABC protocol and SFS policy

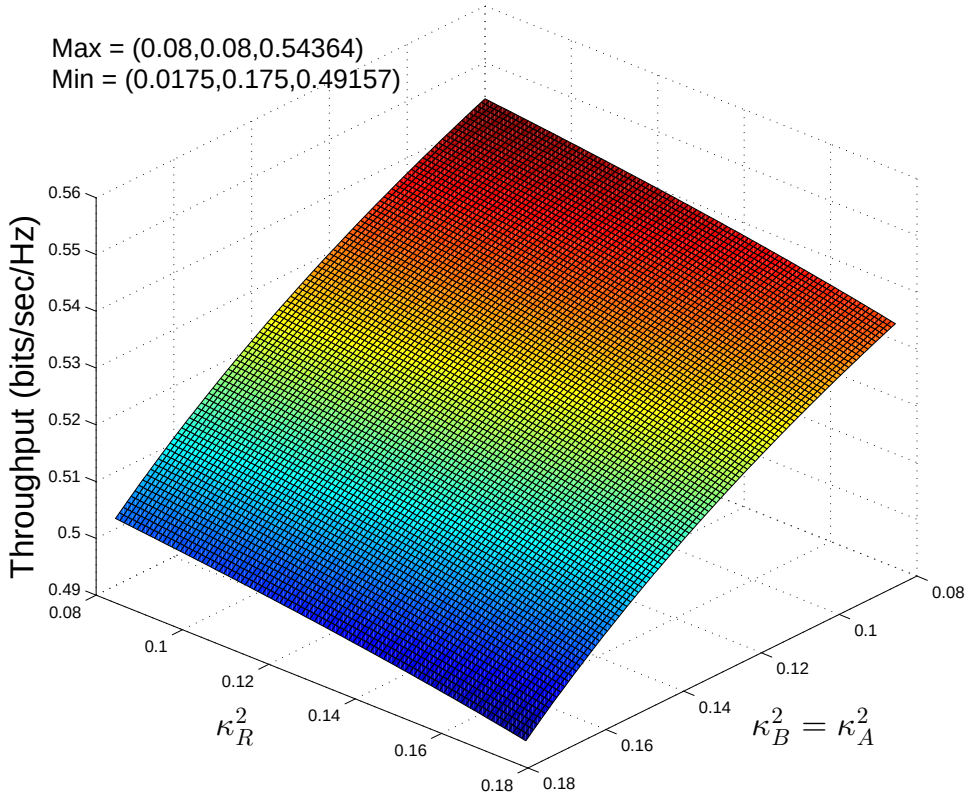

Figure 3.10: The detail impact of hardware impairment at A, B and R on network throughput when $SNDR = 5dB$ with TDBC protocol and DS policy

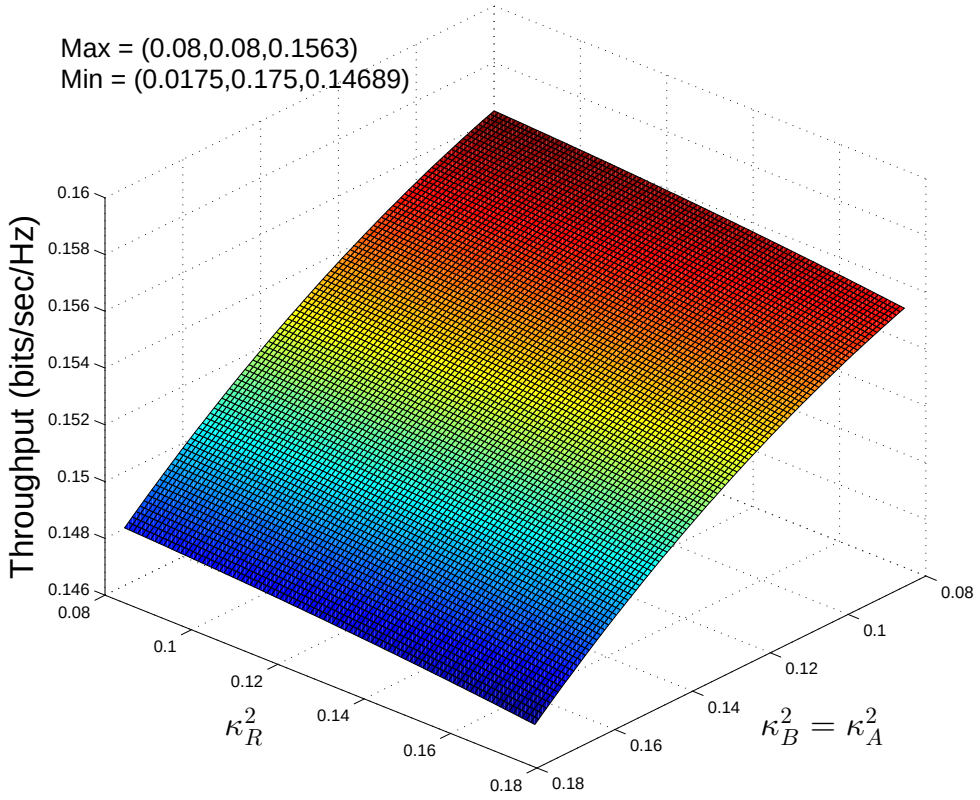

Figure 3.11: The detail impact of hardware impairment at A, B and R on network throughput when $SNDR = 5dB$ with TDBC protocol and SFS policy

impairment levels of transceiver at A, B and R are also satisfy the EVMs requirement of 3GPP LTE, $\kappa_A^2, \kappa_B^2, \kappa_R^2 \in [0.08, 0.175]$. We assume that the hardware quality of the controller center A and sensor B are similar but different from the hardware quality of relay node R ($\kappa_A^2 = \kappa_B^2 \neq \kappa_R^2$). As anticipated, the network throughput peaks at the minimum level of impairments at node A, B and R whereas its nadir establishes at the maximum level of impairments at the three nodes for all four observed network configurations. It can be seen that the hardware impairment level of node A and B has make a greater impact on throughput than that of the relay node R, in particular the impact of transceiver impairments of A and B are three times greater than that caused by relay node for the network with MABC-DS configuration. Therefore, in practice, we can implement the relay node with a low-cost hardware but the hardware quality for controller station A and sensor node B have to be higher than the quality of the relay node R. We also can conclude an important design guideline that network performances can be improved even with low-cost hardware relays.

3.6 Conclusion

This chapter has analyzed the performance of two-way DF wireless sensor networks with imperfect energy harvesting relay nodes. Our analysis has provided engineering insights of self-powered DF TWCR networks: for instance, it was found that MABC with DS energy harvesting provides the best throughput albeit at the expense of implementation complexity. On the other hand, TDBC with SFS offers a simpler solution but with lower throughput. Moreover, it was also confirmed that transceiver impairment deteriorates system performance. The degradation has been quantified as a function of the level of hardware impairments of the controller station, the sensor node and the relay node. We confirm the fundamental capacity limit for the network with four combination given the fixed transmission rate at the controller station and the sensor node. Moreover, we put forward a hardware selection strategy for network implementation where the relay node can employ lower cost hardware than the controller station and the sensor. This conclusion encourage network designers implement relay nodes to improve network performance even with low-cost relays.

4. Soft Information Relaying Protocol

This chapter demonstrates the impact of transceiver impairments on channel capacity and BER performance of a dual-hop half-duplex cognitive relay network over AWGN channel. We consider the SIR protocol where the relay node computes the reliabilities (soft) of the received signal from source and then forwards to the destination. The hardware impairment model of the received signal via AWGN channel is first introduced. The analysis on capacity and BER performance are then presented for the network with BPSK modulation. Furthermore, the impacts of hardware impairments on BER are quantified for the network with SIR and hard DF protocol. The simulation results on channel capacity of the network with SIR protocol acknowledge the ceiling capacity of the realistic transceivers that can not be exceeded by increasing transmit power. Moreover, we found that the BER performance of SIR network with the worst hardware impairment level in 3GPP LTE requirements is on par with the best transceiver level of the network with hard DF. This concludes that the SIR outperforms the hard DF on limit the impact of hardware impairments on BER performance.

4.1 Introduction

Cooperative communication is a promising technique to realize spatial diversity and increased spectral efficiency through user cooperation [15]. There are three basic memoryless relay protocols: amplify-and-forward (AF), decode-and-forward (DF) and estimate-and-forward (EF). In DF, the error propagation can be avoided using decoder process under good channel conditions. However, error-prone relays can destroy the performance of the destination's decoder when the relay forwards

erroneous signals to the destination. In contrast, the AF protocol suffers from the problem of noise amplification. However, estimate and forward (EF) [41]-[42] relay combine the advantages presented in these two protocols and mitigate the shortcomings of traditional protocols such as error propagation to the destination (DF) and noise amplification at the relay (AF).

In [41]–[42], a soft-input soft-output (SISO) encoder was implemented at the relay. However, in [41], the recursive structure of this encoder means that the reliability of the recursively encoded soft bits depends strongly on the least reliable input bits, causing a decaying LLR profile. A scheme for soft parity generation was recently proposed in [43] which has the advantage that successively generated soft symbols do not converge to zero as happens with many existing soft forwarding methods; this method is specific to BPSK.

Cognitive radio is a strong candidate to combat the scarcity of frequency spectrum. In order to protect quality-of-service of primary transmission, the transmit power of secondary users (SUs) should be limited to the maximum interference allowance of primary users (PUs). To tackle this limitation, the idea of two-way cognitive relay (TWCR) networks has been investigated in [30; 31] among others. The cognitive relay networks exploit the advantages of relaying protocols and cognitive radios and are able to overcome the transmit power limits to further boost the system performance.

In [22], the OP of DF cognitive relay networks was reported with the constraint imposed on the interference suffered by the primary users. The work in [19] analyzed the performance of spectrum sharing AF in the existence of transmit power constrain and the interference from a primary transmitter. The OP of the cognitive DF networks over Nakagami-m fading was performed in [23]. In these literature, the transceiver of the relay nodes were supposed to be flawless. Nevertheless, the practical transceiver hardware suffers from several types of impairments; such as, I/Q imbalance [24; 25], high power amplifier non-linearities [26]. Recently, the impacts of hardware impairments to relay networks were provided in [27]. Undoubtedly, those impairments also degrade the system performances of the CR networks, especially when the power budget is high.

We apply the SIR protocol for a cognitive network and evaluate the impact of

transceiver imperfections on channel capacity and BER performance by utilizing the generalized impairment model of [13].We also compare those performance of the SIR protocol to the hard DF protocol in order to confirm the advantages of the SIR protocol. The contributions can be befound in this chapter include:

- We portray SIR protocol for cognitive relay networks and simplify the impairment model for AWGN channel.
- We provide new analysis results for channel capacity and BER performance of the network with SIR protocol under the impact of hardware impairments.
- Finally, we present simulation results which show significant benefits of the SIR scheme compared to hard DF protocol.

Firstly, we describe how to simplify the transceiver hardware impairments model for AWGN channel. It is assumed that the source transmits a signal $x \in \mathbb{C}$ with power P over the wireless channel to the receiver with AWGN noise η that has zero mean and variance $\sigma_\eta^2 = N_0$. The practical transceiver impairments at the source distort the signal x before it is emitted, whilst the imperfect transceiver hardware of the receiver distorts the received signal during the reception phase. Each source of distortion is represented by a different hardware model. Let τ_1, τ_2 be the distortion affecting the source and destination, respectively. The received signal can be succinctly expressed as

$$y = \sqrt{P}(x + \tau_1) + \tau_2 + \eta. \tag{4.1}$$

As in [14], $\tau_1 \sim \mathcal{CN}(0, \kappa_1^2)$ and $\tau_2 \sim \mathcal{CN}(0, \kappa_2^2 P)$, where κ_1, κ_2 are the *impairment levels* at the source and destination transceivers, respectively. Following [14], the distortion powers caused by transceiver impairments at the source and destination can be, more compactly, represented by an *aggregate distortion* power at the receiver, such that $\tau \sim \mathcal{CN}(0, \kappa^2)$, where $\kappa \triangleq \sqrt{\kappa_1^2 + \kappa_2^2}$ is the *aggregate impairment* level. Then, (4.1) can be rewritten as

$$y = \sqrt{P}(x + \tau) + \eta = \sqrt{P}x + \sqrt{P}\tau + \eta, \tag{4.2}$$

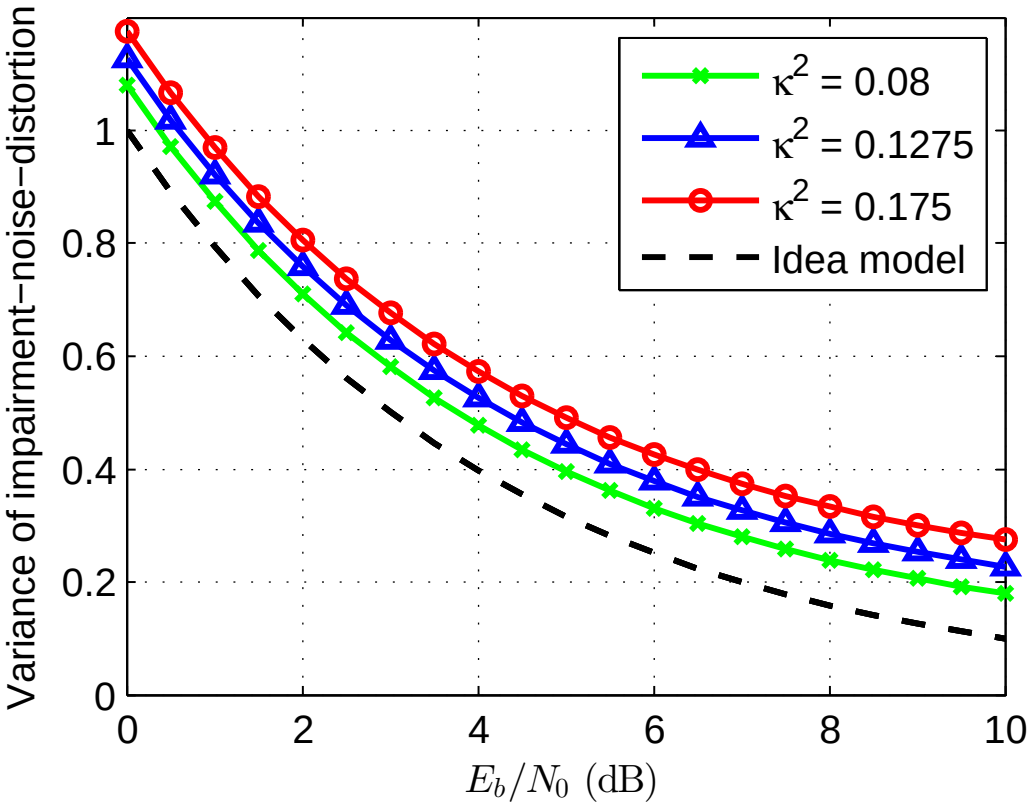

Figure 4.1: Variance of impairment-noise-distortion when transmit power $P = 1$ for difference impairments levels $\kappa^2 \in [0.08; 0.1275; 0.175]$

we define $\varepsilon = \sqrt{P}\tau + \eta$ as the *impairment-noise-distortion*, where $\varepsilon \sim \mathcal{CN}(0, \kappa^2 P + N_0)$. We can rescript (4.2) as

$$y = \sqrt{P}x + \varepsilon. \tag{4.3}$$

As definition of SNR, $\frac{E_b}{N_0} = \frac{P}{\sigma_\eta^2}$, then the variance of ε is given by:

$$\sigma_\varepsilon^2 = \sigma_\eta^2 + \sigma_\tau^2 = P\frac{N_0}{E_b} + \kappa^2 P. \tag{4.4}$$

Fig. 4.1 illustrates the impact of transceiver hardware impairments on variance of the total noise include AWGN and impairment-noise-distortion. It can be seen in Fig. 4.1, σ_ε^2 increases as the rise of the impairment level κ^2. We note that the transmit power is kept unchanged as $P = 1$ in order to obtain the simulation results in Fig. 4.1 while the hardware impairment level in the range $\kappa \in [0.08, 0.175]$

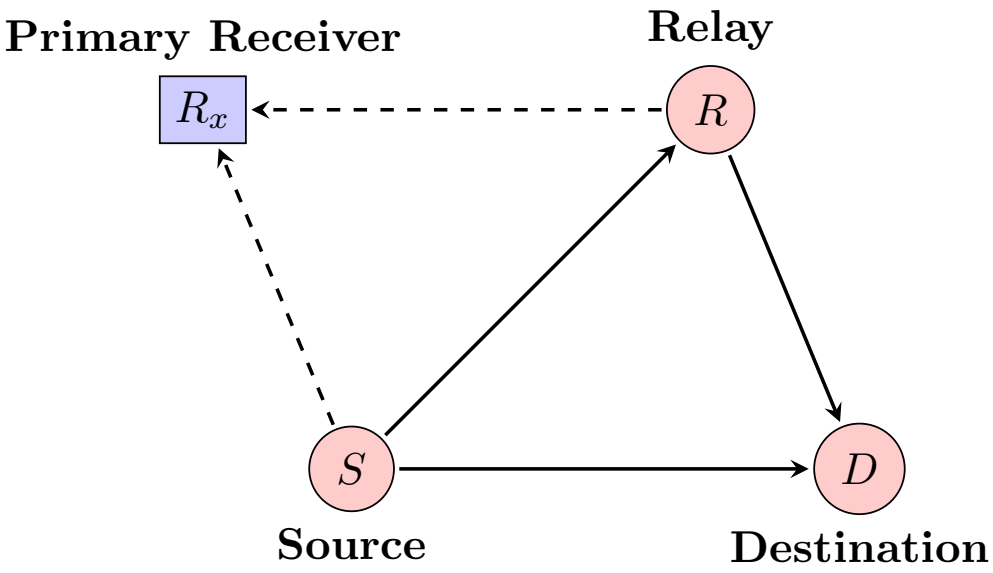

Figure 4.2: A three-node cognitive relay network.

are examined, which resemble the error vector magnitudes (EVMs) of 3GPP LTE requirements.

4.2 System and channel model

In this chapter, we consider a half-duplex cognitive three-node relay channel as illustrated in Fig. 4.2. In this cognitive relay network, the source node (S) transmits information x to the destination node (D) with the help of the relay node (R). R_x is a receiver in the primary network. We assume each node is equipped with a single antenna and working in half-duplex mode. To protect Rx from interference signals caused by the transmission of the cognitive users, we define I_P as the maximum tolerance interference received at Rx. We observe a case where the cognitive users are allowed to transmit with peak power, hence, the transmit power at S and R are I_P.

The information is conveyed in two timeslots; in the first timeslot, S broadcasts x to both R and D. The received information y_{SR} is processed using the relay function $f(y_{SR})$, and then it is forwarded to D via R. All channels of the network

are assumed to be AWGN channel. Without loss of generality, the additive noise terms η_i, $i \in \{S,R,D\}$, is assumed to have zero mean and variance σ_i^2, such that $\eta_i \sim \mathcal{CN}(0,\sigma_i^2)$. Moreover, following the discussion in the previous section, the aggregate impairment level at R and D are presented as κ_R^2 and κ_D^2, respectively. We consider the BPSK modulation, $x \in \{\pm 1\}$ to simplify the analysis, however our results can be easily extended to higher order modulations.

Thus, the received signals in the first timeslot at R and D with transmit power P_S can be respectively expressed as

$$y_{SR} = \sqrt{I_P}x + \varepsilon_R = \sqrt{P_S}x + \varepsilon_R, \tag{4.5}$$

$$y_{SD} = \sqrt{I_P}x + \varepsilon_D = \sqrt{P_S}x + \varepsilon_D, \tag{4.6}$$

where the impairment-distortion-noise at R and D are $\varepsilon_j \sim \mathcal{CN}(0, \kappa_j^2 P_k + N_0)$, where $j \in \{R,D\}$ and $k \in \{S,R\}$. In the second timeslot, the received signal at D can be written as

$$y_{RD} = \sqrt{P_R} f(y_{SR}) + \varepsilon_D = \sqrt{P_R} x_R + \varepsilon_D. \tag{4.7}$$

4.3 Soft information relaying

We employ the soft information relaying protocol in the cognitive relay network while the hard decode-and-forward protocol is used as a bench mark to evaluate the benefits of the SIR protocol under hardware impairments.

4.3.1 Calculation of soft information at relay node

In the first timeslot, source transmits signal $\boldsymbol{x}$ to relay. The relay calculates and forwards the MMSE value of this received signal y_{SR} to D. The conditional expectation of $\boldsymbol{x}$ is $(\mathbb{E}[x|y_{SR}])$, which is calculated as

$$\widetilde{x_R} = \mathbb{E}[x|y_{SR}] = \tanh\left(\frac{L_R}{2}\right), \tag{4.8}$$

where $L_R = \ln \frac{p(y_{SR}|x=1)}{p(y_{SR}|x=-1)}$ is *a log-likelihood ratio* (LLR) of the received symbol x with BPSK modulation and $\tanh(t) = \frac{e^{2t}-1}{e^{2t}-1}$ is the hyperbolic tangent function. Therefore, the relay function can be expressed as

$$f(y_{SR}) = \frac{\tanh\left(\frac{L_R}{2}\right)}{\sqrt{\mathbb{E}\left[\tanh\left(\frac{L_R}{2}\right)\right]}} = \beta \widetilde{x}_R, \tag{4.9}$$

where $\beta = \sqrt{\mathbb{E}\left[\tanh\left(\frac{L_R}{2}\right)\right]}$. In practice the factor β is chosen to satisfy the transmit power constraint at the relay, i.e.,

$$\beta = \sqrt{\frac{1}{\frac{1}{N}\sum_{i=1}^{N} \tilde{x}_i^2}}, \tag{4.10}$$

where N is the number of symbols.

4.3.2 Calculation of LLR at the destination

In the second timeslot, the relay forwards the soft information of the received signal in the first timeslot to the destination. Hence, the destination receives two different signals via two independent channels, i.e., y_{SD} and y_{RD}. First, the LLR value of the received signal y_{SD} is calculated as

$$L_{SD} = \ln \frac{p(y_{SD}|x=1)}{p(y_{SD}|x=-1)} = \frac{2y_{SD}}{\sigma_{\varepsilon_D}^2}. \tag{4.11}$$

Assume that the received version of the soft symbol x_R at the destination is $\widetilde{x}_R$. From (4.7), the soft information at D can be rewritten as

$$y_{RD} = \sqrt{P_R}\beta \widetilde{x}_R + \varepsilon_D. \tag{4.12}$$

The transmit power P_R is selected to satisfy $P_R \leq \frac{I_P}{\beta^2}$. The relationship between the soft symbol at R, $\widetilde{x}_R$, and the correct symbol x_R, is modeled in [41] as

$$\widetilde{x}_R = x_R(1-\widetilde{\eta}), \tag{4.13}$$

where $\widetilde{\eta}$ is the *soft noise* random variable whose mean and variance are measured offline and respectively given by

$$\mu_{\widetilde{\eta}} = \frac{1}{N}\sum_{k=1}^{N} |\widetilde{x}_R^k - x_R^k|, \tag{4.14}$$

$$\sigma_{\widetilde{\eta}}^2 = \frac{1}{N}\sum_{k=1}^{l} (1 - \widetilde{x}_R^k x_R^k - \mu_{\widetilde{\eta}})^2. \tag{4.15}$$

We denote that $\mu_{\widetilde{\eta}}$ and $\sigma_{\widetilde{\eta}}^2$ are priorly computed and stored at D for calculating LLR in real time transmission. Hence, (4.12) can be recast as

$$\begin{aligned} y_{RD} &= \sqrt{P_R}\beta\left[x_R(1-\widetilde{\eta}+\mu-\mu)\right] + \varepsilon_D \\ &= \sqrt{P_R}\beta x_R(1-\mu) - \sqrt{P_R}\beta x_R(\mu+\widetilde{\eta}) + \varepsilon_D \\ &= \sqrt{P_R}\beta x_R(1-\mu) + \bar{\eta}_D \end{aligned} \tag{4.16}$$

In (4.16), $\bar{\eta}_D = -\sqrt{P_R}\beta x_R(\mu+\widetilde{\eta}) + \varepsilon_D$ is the noise term of the received signal at D form R in the second timeslot. This equivalent noise is not a Gaussian random variable. However, its distribution has zero mean and variance is derived as

$$\sigma_{\bar{n}}^2 = P_R\beta^2(\mu+\widetilde{\eta})^2 + \varepsilon_D^2. \tag{4.17}$$

Therefore, the LLR of the received signal y_{RD} can not be obtained as (4.11) because the probability density function of the soft symbol is unknown. The LLR of y_{RD} is approximated using the soft noise model as follows

$$L_{RD} = \ln\frac{p(x=1|y_{RD})}{p(x=-1|y_{RD})} = \frac{2(1-\mu_{\widetilde{\eta}})}{P_R\sigma_{\widetilde{\eta}}^2\beta^2 + \sigma_{\varepsilon_D}^2} y_{RD}. \tag{4.18}$$

From (4.11) and (4.18), the total LLR of the received signal at D in two different channel routes is computed as

$$L_D = L_{SD} + L_{RD}. \tag{4.19}$$

The decoded signal at D is

$$\hat{x}_D = \text{sign}(L_D). \tag{4.20}$$

4.4 Numerical results and discussion

In this section, we present the performance of the SIR protocol for the three-node cognitive relay network under the impact of transceiver hardware impairments.

4.4.1 Simulation parameters

We consider the cognitive relay network where data is transmitted using BPSK modulation. The interference allowance power is assumed to be satisfy where transmit power at source and relay are assumed to be $P_S = P_R = 1$. Encoders and decoders are supposed to be ideal hardware, however wireless transceivers are modeled with hardware impairment level is in the range $[0.08, 0.175]$. Unless otherwise states, the aggregate impairment levels of the relay and destination are similar, i.e. $\kappa_R^2 = \kappa_D^2 = \kappa^2$.

Table 4.1: Simulation parameters for the soft information relaying protocol

Name	**Value**
Fading model	AWGN
Modulation scheme	BPSK
Outage threshold	$\gamma_t = 3$
Hardware impairment level	$\kappa_R^2, \kappa_D^2, \kappa^2 \in [0.08, 0.175]$
Maximum transmit power	$P_S = P_R = 1$

4.4.2 Channel capacity in AWGN performance

From (4.6) and (4.16), we have the SNR of the received signals at D from two timeslots are respectively given by

$$\gamma_{SD} = \frac{P_S}{\sigma_{\varepsilon_D}^2} = \frac{I_P}{\sigma_{\varepsilon_D}^2}, \quad \gamma_{SR} = \frac{P_S}{\sigma_{\varepsilon_R}^2} = \frac{I_P}{\sigma_{\varepsilon_R}^2}, \tag{4.21}$$

$$\gamma_{RD} = \frac{P_R \beta^2}{\sigma_{\tilde{n}_D}^2} = \frac{I_P}{\sigma_{\tilde{n}_D}^2} = \frac{I_P}{I_P \sigma_{\tilde{\eta}}^2 + \sigma_{\varepsilon_D}^2}. \tag{4.22}$$

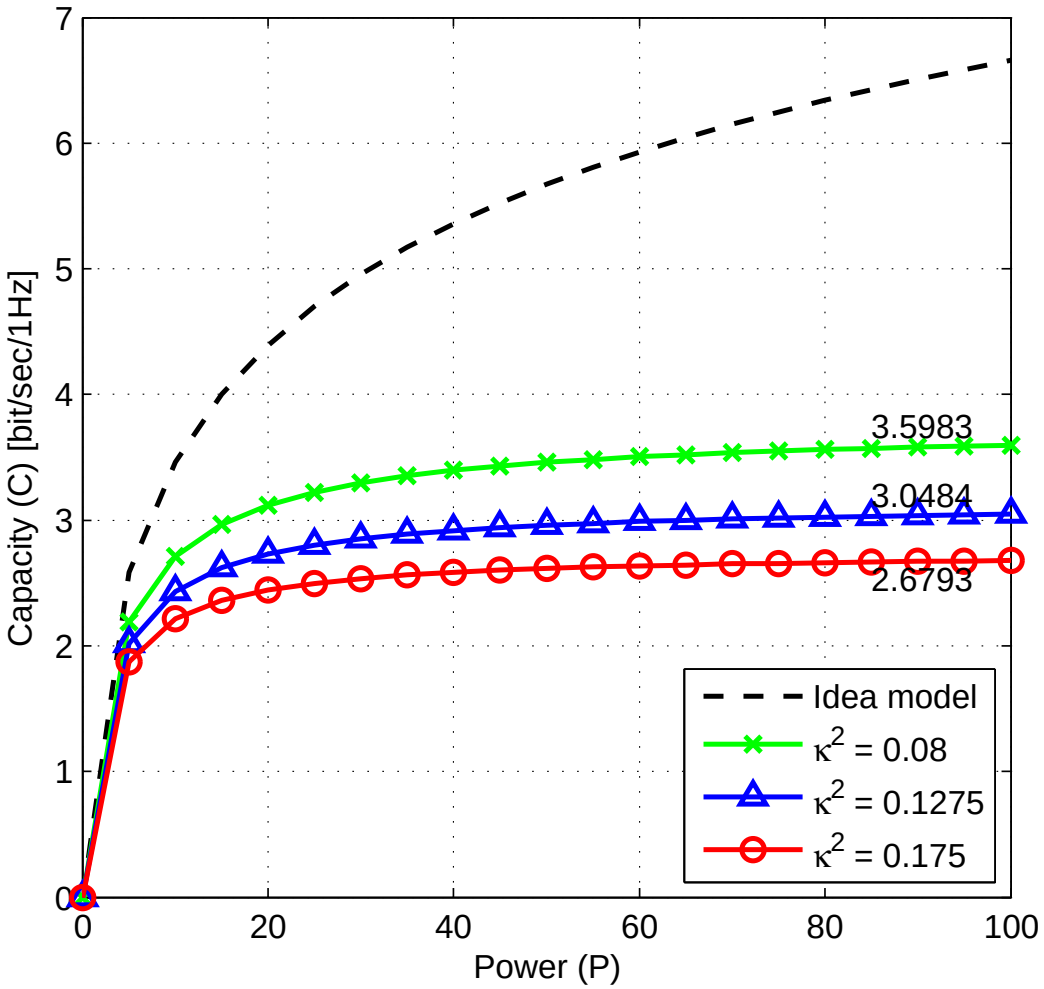

Figure 4.3: Capacity performance of the network when the bandwidth $B = 1$ (Hz), variance noise $\sigma_\eta^2 = 1$ and $\kappa^2 = [0, 0.08, 0.125, 0.175]$.

The end-to-end SNR of the network is obtained as

$$\gamma_D = \max\left(\min(\gamma_{SR}, \gamma_{RD}), \gamma_{SD}\right). \tag{4.23}$$

The capacity of AWGN channel with bandwidth B is given by Shannon's well-know formula

$$C = B\log_2(1 + \frac{\gamma_D}{B}). \tag{4.24}$$

Fig. 4.3 demonstrates the capacity of the cognitive relay network with SIR proto-

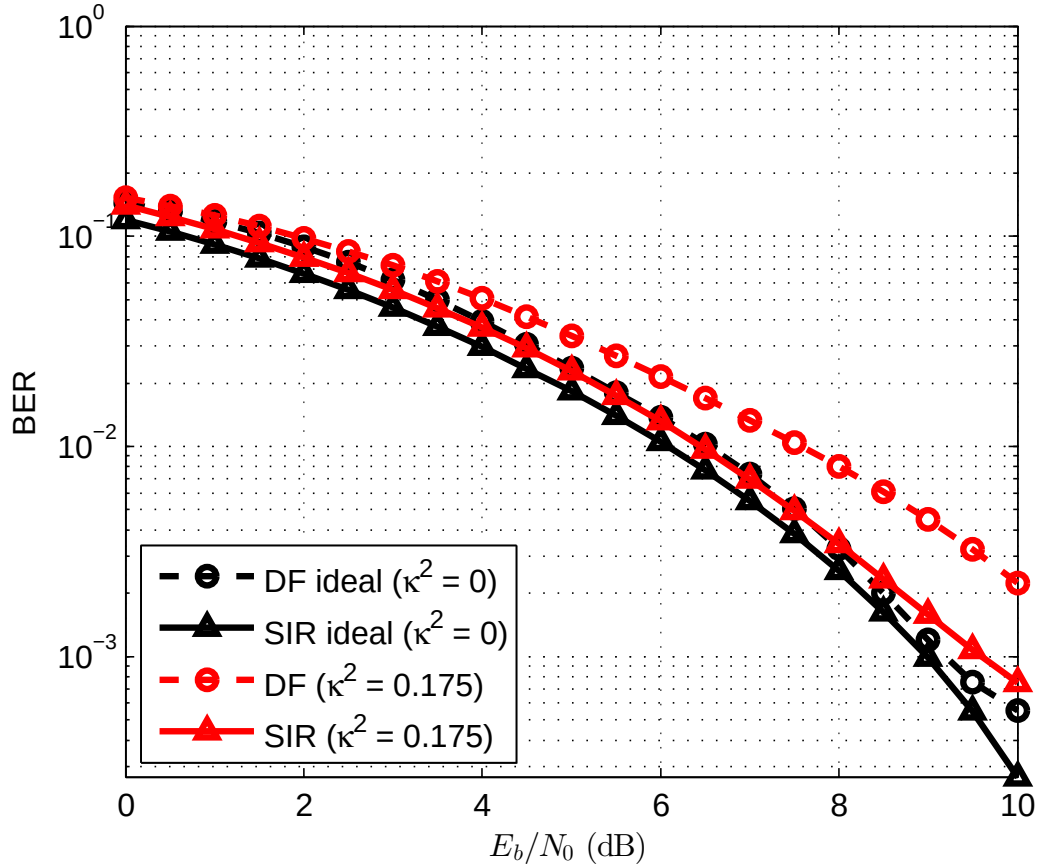

Figure 4.4: BER performance for the SIR protocol in compared to DF protocol over AWGN channel for ideal transceiver and realistic transceiver model with hardware impairment level $\kappa^2 = 0.175$.

col versus transmit power P for different transceiver impairment levels κ^2. It can be seen that the capacity of the channel for ideal transceiver ($\kappa^2 = 0$) is theoretically unlimited when $P \to \infty$. However, for the network with realistic transceiver ($\kappa^2 \neq 0$), the ceiling capacity is established as the growth of transmit power. This is fundamental limit for the network spectral efficiency. As we observe, the ceiling capacity decreases when the impairment levels increase. In particular, it is about 0.9 (bit/sec/1Hz) lost as κ^2 rises from 0.08 to 0.175.

4.4.3 BER performance

Fig. 4.4 compares the BER performance of the cognitive relay network over AWGN channel of the SIR relaying scheme with that of hard DF protocol. The SNRs of $S \to R$, $S \to D$ and $R \to D$ wireless link are assumed to equal and rise in the range $[0, 10]$ dB to represent both poor and good channel conditions.

Overall, the network with SIR scheme outperforms that with DF scheme in term of BER; BER increases as the growth of hardware impairment level κ^2, especially when SNR is high. It is noticed that BER of the network with SIR protocol with $\kappa^2 = 0.175$ is on par with that of the DF network with ideal transceiver and just under the performance of the SIR network with perfect transceiver. In particular, BER of the DF network falls sharply in the high SNR regime, from 7×10^{-4} to 20×10^{-4} when κ^2 increases from 0 (idea transceiver) to 0.175; whereas it reduces gradually by 4.5×10^{-4} for the network with SIR relaying protocol.

This explains that the the SIR protocol is more effective to remove the impact of noise that the DF protocol albeit at the expense of implementation complexity of the noise variance computation circuit. This evidence claim that cognitive relay network with SIR scheme outperforms the network with the DF protocol; moreover, SIR protocol is able to discard the impact of transceiver impairment when compared with the DF protocol.

4.5 Conclusion

This research has presented the simulation results of BER and capacity performance under the impact of hardware impairments of a cognitive relay network using SIR protocol. Our numerical results demonstrated that the SIR protocol outperforms the hard DF scheme. Interestingly, BER of the SIR network with transceiver hardware impairment level $\kappa^2 = 0.175$ is on par with that of the DF protocol with perfect transceiver $\kappa^2 = 0$. Hence, SIR protocol can be employed on the terminal wireless devices to mitigate the impacts of the transceiver hardware impairments. Furthermore, the fundamental limit achievable capacity of wireless terminal with realistic

transceiver hardware impairment model has been found. The ceiling capacity is established even the transmit power increase to infinity.

5. Overall Conclusion and Future Work

This work has accomplished the goals of analyzing the impact of transceiver hardware impairment on the end-to-end reliability and throughput of cognitive networks in various relaying protocols, which was presented in Chapter 1 and Chapter 2. Furthermore, a case study of two-way cognitive sensor network with wireless energy harvesting relay node has been examined for the purpose of bringing the research results into life that was explained in Chapter 3. The analysis provided the detail outage probability and achievable through as well as the suggestion of performance and implementation cost trade-off for each network configuration. In Chapter 4, the soft information relaying scheme is presented and the analysis results put forward a conclusion that this relaying protocol can mitigate the influence of the impact on a similar quality transceiver hardware. In particular, the contributions of this dissertation can be categorized into three main-folds:

1. This work introduces the general transceiver hardware impairment model. By utilizing this model in the analysis, the gap in network performance that created by simulating and the realistic implementation can be narrowed.
2. The performance analysis of the end-to-end outage probability and network throughput of cognitive relay networks in the presence of transceiver hardware impairment model have been presented along with the important insights and discussion.
3. A new analysis results of soft information relaying protocol shows that it can reduce the impact of transceiver hardware impairments in cognitive relay networks.

The results of system performance of the soft information relaying protocol was given in this work is deserved to be studied deeper. As such, improving the cognitive network topology in which multiple relay nodes are employed with soft information relaying protocol can be considered as a direction to extend this research. In addition, the study on improving error model of the received signal at the destination is also a good topic of future work.

In conclusion, multihop wireless network, including relay and cognitive relay network, is a realization of future wireless network where the cost of hardware and frequency bands usage is effective. Hence, it may expedite the goal of ubiquitous wireless network in a way that we will be surprised.

References

[1] R.-G. Cheng, "Introduction to opportunity driven multiple access (odma)," *IEEE C802. 16mmr-05*, vol. 12, 2002.

[2] V. Genc, S. Murphy, Y. Yu, and J. Murphy, "Ieee 802.16j relay-based wireless access networks: An overview," *IEEE Trans. Wireless Commun.*, vol. 15, no. 5, pp. 56–63, Oct. 2008.

[3] "Government policy on frequency bands in japan," http://www.softbank.jp/annual-reports/2013/en/segmentinformation/marketdata/frequencyadministrationjapan.html, accessed: 2015-11-21.

[4] H. Hojo, "Trends in wireless access system technology toward expanded broadband based on optical and wireless systems," *NTT Tsukuba Forum 2007 Workshop Lectures 3*, vol. 6, no. 5, May 2002.

[5] J. Mitola and G. Q. Maguire, "Cognitive radio: Making software radios more personal," *IEEE Pers. Commun.*, vol. 6, no. 4, pp. 13–18, Aug. 1999.

[6] L. M. Correia and R. Prasad, "An overview of wireless broadband communications," *IEEE Commun. Mag.*, vol. 35, no. 1, pp. 28–33, Jan. 1997.

[7] P. Smulders, "Exploiting the 60 ghz band for local wireless multimedia access: prospects and future directions," *IEEE Commun. Mag.*, vol. 40, no. 1, pp. 140–147, Aug. 2002.

[8] C. Muschallik, "Influence of rf oscillators on an ofdm signal," *IEEE Trans. Consum. Electron.*, vol. 41, no. 3, pp. 592–603, Aug. 1995.

[9] T. Pollet, M. Van Bladel, and M. Moeneclaey, "Ber sensitivity of ofdm systems to carrier frequency offset and wiener phase noise," *IEEE Trans. Commun.*, vol. 43, no. 2/3/4, pp. 191–193, Feb./Mar./Apr. 1995.

[10] L. Piazzo and P. Mandarini, "Analysis of phase noise effects in ofdm modems," *IEEE Trans. Commun.*, vol. 50, no. 10, pp. 1696–1705, May 2002.

[11] A. Abidi *et al.*, "Direct-conversion radio transceivers for digital communications," *IEEE J. Solid-State Circuits*, vol. 30, no. 12, pp. 1399–1410, Dec. 1995.

[12] B. Razavi, "Design considerations for direct-conversion receivers," *IEEE Trans. Circuits Syst. II*, vol. 44, no. 6, pp. 428–435, 1997.

[13] S. Tim, *RF Imperfections in High-Rate Wireless Systems : Impact and Digital Compensation*. Springer Publishing, 2010.

[14] M. Matthaiou, A. Papadogiannis, E. Björnson, and M. Debbah, "Two-way relaying under the presence of relay transceiver hardware impairments," *IEEE Commun. Lett.*, vol. 17, no. 6, pp. 1136–1139, Jun. 2013.

[15] J. N. Laneman, D. N. Tse, and G. W. Wornell, "Cooperative diversity in wireless networks: Efficient protocols and outage behavior," *IEEE Trans. Inf. Theory*, vol. 50, no. 12, pp. 3062–3080, Dec. 2004.

[16] L. Luo, P. Zhang, G. Zhang, and J. Qin, "Outage performance for cognitive relay networks with underlay spectrum sharing," *IEEE Commun. Lett.*, vol. 15, no. 7, pp. 710–712, Jul. 2011.

[17] K. J. Kim, T. Duong, and H. Poor, "Outage probability of single-carrier cooperative spectrum sharing systems with decode-and-forward relaying and selection combining," *IEEE Trans. Wireless Commun.*, vol. 12, no. 2, pp. 806–817, Feb. 2013.

[18] R. H. Louie, Y. Li, and B. Vucetic, "Practical physical layer network coding for two-way relay channels: performance analysis and comparison," *IEEE Trans. Wireless Commun.*, vol. 9, no. 2, pp. 764–777, Feb. 2010.

[19] T. Duong, V. N. Q. Bao, H. Tran, G. C. Alexandropoulos, and H.-J. Zepernick, "Effect of primary network on performance of spectrum sharing AF relaying," *Electronics letters*, vol. 48, no. 1, pp. 25–27, Jan. 2012.

[20] T. Q. Duong, P. L. Yeoh, V. N. Q. Bao, M. Elkashlan, and N. Yang, "Cognitive relay networks with multiple primary transceivers under spectrum-sharing," *IEEE Signal Process. Lett.*, vol. 19, no. 11, pp. 741–744, Nov. 2012.

[21] Y. Hua, D. W. Bliss, S. Gazor, Y. Rong, and Y. Sung, "Guest editorial theories and methods for advanced wireless relays - Issue I," *IEEE J. Sel. Areas Commun.*, vol. 30, no. 8, pp. 1297–1303, Aug. 2012.

[22] Y. Guo, G. Kang, N. Zhang, W. Zhou, and P. Zhang, "Outage performance of relay-assisted cognitive-radio system under spectrum-sharing constraints," *Electronics Letters*, vol. 46, no. 2, pp. 182–184, Jan. 2010.

[23] C. Zhong, T. Ratnarajah, and K.-K. Wong, "Outage analysis of decode-and-forward cognitive dual-hop systems with the interference constraint in nakagami-fading channels," *IEEE Trans. Veh. Technol.*, vol. 60, no. 6, pp. 2875–2879, July 2011.

[24] Y. Zou, M. Valkama, and M. Renfors, "Digital compensation of I/Q imbalance effects in space-time coded transmit diversity systems," *IEEE Trans. Signal Process.*, vol. 56, no. 6, pp. 2496–2508, June 2008.

[25] J. Qi, S. Aïssa, and M.-S. Alouini, "Analysis and compensation of I/Q imbalance in amplify-and-forward cooperative systems," in *Proc. IEEE WCNC*, Apr. 2012, pp. 215–220.

[26] J. Qi and S. Aïssa, "On the power amplifier nonlinearity in MIMO transmit beamforming systems," *IEEE Trans. Commun.*, vol. 60, no. 3, pp. 876–887, Mar. 2012.

[27] E. Björnson, M. Matthaiou, and M. Debbah, "A new look at dual-hop relaying: performance limits with hardware impairments," *IEEE Trans. Commun.*, vol. 61, no. 11, pp. 4512–4525, Nov. 2013.

[28] I. Suliman, L. Janne, B. Timo, and U. Kenta, "Analysis of cognitive radio networks with imperfect sensing," *IEEE Trans. Commun.*, vol. 96, no. 6, pp. 1605–1615, Jun. 2013.

[29] P. Herath, U. Gunawardana, R. Liyanapathirana, and N. Rajatheva, "Outage probability analysis of multiple antenna dual-hop networks with interference-limited relay," *IEICE transactions on communications*, vol. 96, no. 2, pp. 577–584, Feb. 2013.

[30] L. Yang, M.-S. Alouini, and K. Qaraqe, "On the performance of spectrum sharing systems with two-way relaying and multiuser diversity," *IEEE Commun. Lett.*, vol. 16, no. 8, pp. 1240–1243, Aug. 2012.

[31] K. Kim, T. Q. Duong, M. Elkashlan, P. L. Yeoh, and A. Nallanathan, "Two-way cognitive relay networks with multiple licensed users," in *Proc. IEEE GLOBECOM*, Dec. 2013, pp. 992–997.

[32] X. Zhang, Z. Zhang, J. Xing, R. Yu, P. Zhang, and W. Wang, "Exact outage analysis in cognitive two-way relay networks with opportunistic relay selection under primary user's interference," *IEEE Trans. Veh. Technol.*, vol. 64, no. 6, pp. 2502–2511, June 2015.

[33] S. Petros and H. Dimitrios, "Cognitive networking in a self-powered wireless sensor network testbed," in *MOBICOM*. Vancouver, BC: IEEE, Sep. 2014, pp. 4775–4780.

[34] J. Li, M. Matthaiou, and T. Svensson, "I/Q imbalance in two-way AF relaying," *IEEE Trans. Commun.*, vol. 62, pp. 2271 – 2285, Jul. 2014.

[35] A. A. Nasir, X. Zhou, S. Durrani, and R. A. Kennedy, "Relaying protocols for wireless energy harvesting and information processing," *IEEE Trans. Wireless Commun.*, vol. 12, no. 7, pp. 3622–3636, July 2013.

[36] B. Medepally and N. B. Mehta, "Voluntary energy harvesting relays and selection in cooperative wireless networks," *IEEE Trans. Wireless Commun.*, vol. 9, no. 11, pp. 3543–3553, Nov. 2010.

[37] X. Zhou, R. Zhang, and C. K. Ho, "Wireless information and power transfer: Architecture design and rate-energy tradeoff," in *Proc. IEEE GLOBECOM*, Dec. 2012, pp. 3982–3987.

[38] E. Björnson, P. Zetterberg, and M. Bengtsson, "Optimal coordinated beamforming in the multicell downlink with transceiver impairments," in *Proc. IEEE GLOBECOM*, Dec. 2012, pp. 4775–4780.

[39] S. Luo, R. Zhang, and T. J. Lim, "Optimal save-then-transmit protocol for energy harvesting wireless transmitters," *IEEE Trans. Wireless Commun.*, vol. 12, no. 3, pp. 1196–1207, Mar. 2013.

[40] I. Gradshteyn and I. Ryzhik, *Table of integrals, series and products, 6th edition*. Academic Press, 2000.

[41] Y. Li, B. Vucetic, T. F. Wong, and M. Dohler, "Distributed turbo coding with soft information relaying in multihop relay networks," *IEEE J. Sel. Areas Commun.*, vol. 24, no. 11, pp. 2040–2050, 2006.

[42] S. C, I, L. J, and A. B, "Map detection with soft information in an estimate and forward relay network," in *44th ASILOMAR*, California, USA, 2010, pp. 121–125.

[43] K. J. D, N and F. M, F, "A soft forwarding scheme for an arbitrary signal constellations in cooperative wireless networks," *IEEE Trans. Veh. Technol.*, vol. 99, no. 10, pp. 927–929, May 2015.

Acknowledgments

Standing at this point and looking back over the past three years, it reminds me a mixing feeling of joy and despair. I cherish all those good and hard memories.

First and foremost, I would like to extend my sincere gratitude to my supervisor Prof. Hiroshi Ochi for his continued support. I appreciate your close supervision and essential advice on my research as well as my daily life that I am grateful for being received. I would like to express my sincere thanks to my co-supervisor Prof. Trung Q. Duong for his indispensable supervision on directing me into the interesting research topics, cognitive relay network. I greatly appreciate his generousness in sharing his expertise, research collaborations as well as time on our frequent discussions that have inspired me with new research ideas. Special thanks to Prof. Masayuki Kurosaki, Asst. Prof. Leonardo Lanante, Dr. Yuhei Nagao for the countless support and advice during my study. I would like to express my high appreciation to Dr. Nalin Jayakody, my mentor on soft relaying protocol, for your time, support and patience.

I owe a special thank to my lab mates who always be there when I need help. Thank you very much my research colleagues inside and outside KIT for their kindly support both in technical and mental. I would like to thank to every single friend of mine who made my day for innumerable times. I would cover your names in this limit space but I will delivery my thanks to you in person.

Last but not least, I would like to send my thankful heart to my beloved mom, my family back in Vietnam as well as my dear dad in heaven for their unconditional love and belief. I couldn't make it without you who I am greatly beholden to.

Publications

Journal

1. *Dang Khoa Nguyen*, Hiroshi Ochi, "Two-way Cognitive DF Relaying in WSNs with Practical RF Energy Harvesting Relay Hardware," *IEICE Trans. on Commun.*, Vol.E99-B, No.03, pp.-, Mar. 2016. (to appear)

2. *Dang Khoa Nguyen*, Leonardo Lanate, Hiroshi Ochi, "High Throughput – Resource Saving Hardware Implementation of AES-CCM for Robust Security Network," *Journal of Automation and Control Engineering,* Vol.1, No.3, pp. 250-254, Sep. 2013. doi: 10.12720/joace.1.3.250-254.

International Conference

1. *Dang Khoa Nguyen*, Dushantha Nalin K. Jayakody, Hiroshi Ochi, "Soft Information Relaying with Transceiver Hardware Impairments in Cognitive Networks," in Proc. *International Conference on Information, Communications and Signal Processing (ICICS)*, Special session ID: Th31 – Cooperation in Networks. paper ID: TH31-7, Dec. 2015.

2. *Dang Khoa Nguyen*, Michail Matthaiou, Trung Q. Duong, Hiroshi Ochi, "RF Energy Harvesting Two-way Cognitive DF Relaying with Transceiver Impairments," in Proc. *IEEE International Conference on Communication Workshop (ICCW) on Green Communications and Networks with Energy Harvesting, Smart Grids, and Renewable Energies*, session ID: AM1, paper ID: AM1-5, June, 2015, pp. 1970–1975.

3. *Dang Khoa Nguyen*, Hiroshi Ochi, "Transceiver Impairments in DF/AF Dual-Hop Cognitive Relay Networks: Outage Performance and Throughput Analysis," in Proc. *IEEE 81th Vehicular Technology Conference (VTC)*, session ID: 3P – Cooperative Communications, Distributed MIMO and Relaying, paper ID: 13, May 2015, pp. 1–5.

4. *Dang Khoa Nguyen*, Hiroshi Ochi, "On the Impact of Transceiver Impairments to Cognitive DF Relay Networks," in Proc. *IEEE Asia Pacific Conference on Circuits and Systems (APCCAS)*, session ID: A3P-D – Embedded Systems, Circuits and Systems for Communications, paper ID: A3P-D-04, Nov. 2014, pp. 125-128.

5. *Dang Khoa Nguyen*, Tu Thanh Lam, Hiroshi Ochi, "Performance Analysis: DF Cognitive Network with Transceiver Imperfections," in Proc. *The 48th Annual Asilomar Conference on Signals, Systems and Computers*, session ID: TP8a1 – Cognitive Radio II, paper ID: TP8a1-8, Nov. 2014, pp. 1604-1608.

6. *Dang Khoa Nguyen*, Leoardo Lanante, Yuhei Nagao, Masayuki Kurosaki, Hiroshi Ochi, "Implementation of 2.6 Gbps Super-high Speed AES-CCM Security Protocol for IEEE802.11i," in Proc. *The 13th International Symposium on Communications and Information Technologies (ISCIT 2013)*, session ID: B1-4 – Smart System of Wireless Image Communications, paper ID: S1, Sep. 2013, pp. 669–673.

Technical Report

1. *Dang Khoa Nguyen*, Hiroshi Ochi, "Outage Performance of Cognitive Decode-and-Forward Relaying Networks with Hardware Impairments," in Proc. *Technical Committee on Radio Communication Systems - IEICE*, session ID: RCS2014-150, Aug. 2014, pp. 67–71.

2. *Khoa Dang Nguyen*; Leonardo Lanate; Hiroshi Ochi, "Hardware Implementation of High Speed, Parallel AES-CCMP for Robust Security Network," in Proc. *IEICE General Conference*. Okayama, Japan, session ID: B-5 – Wireless Communication B, paper ID: B-5-141, Mar. 2012.